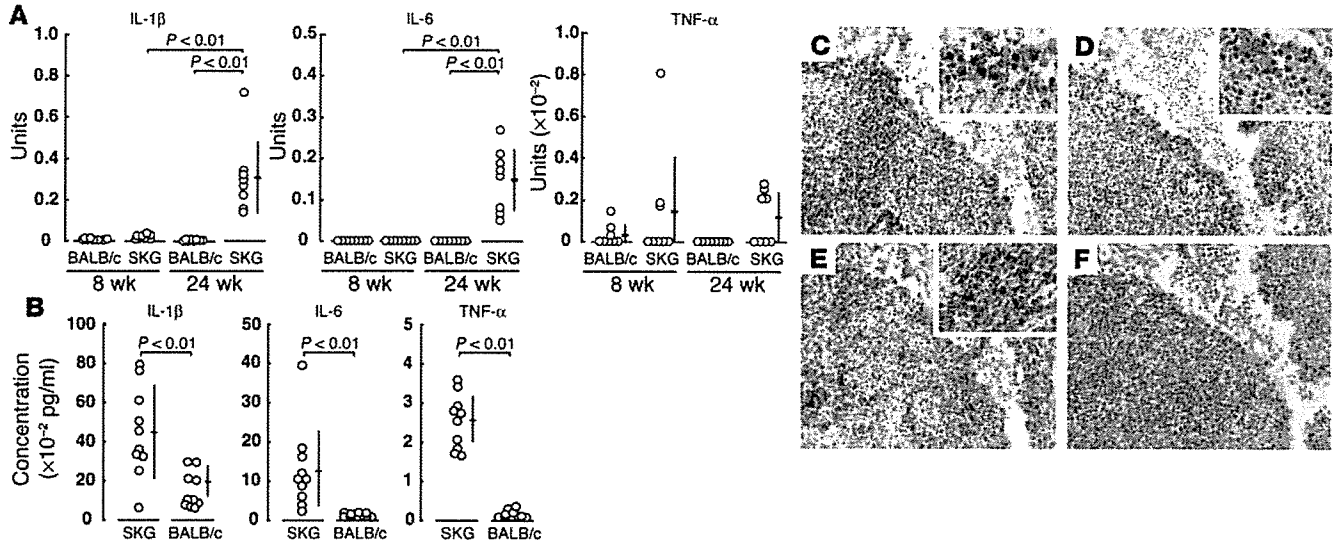

Figure 2

Expression of cytokines at mRNA and protein levels. (**A**) Quantitative RT-PCR for indicated genes was performed with ankle joints from 8- or 24-week-old SKG or BALB/c mice. Bars show the means ± SD. See Methods for the definition of units. (**B**) Concentrations of indicated cytokines, assessed by ELISA, in the joint fluid of 32-week-old SKG and BALB/c mice (n = 10 each). Bars show the means ± SD. (**C–F**) Immunohistochemical staining of the synovial tissue of a finger joint of a 4-month-old SKG mouse for IL-1β (**C**), TNF-α (**D**), or IL-6 (**E**), with staining control (**F**) (original magnification, ×40). Insets show higher magnifications of a part of synovium.

lining cells and scattered in the sublining region (Figure 2E). The localization of IL-6–expressing cells correlated with that of MAC-1$^+$, I-A/I-E$^+$ macrophages or CD4$^+$ cells (Figure 1).

These results collectively indicate that the inflamed synovial tissue of SKG mice actively produces IL-1β, TNF-α and IL-6; the cells forming TNF-α and IL-1β are apparently the same and constitute the superficial lining layer; and the cells mainly forming IL-6 are apparently different from those forming IL-1β and TNF-α and localize differently.

Effect of deficiency in particular cytokines on the development and progression of SKG arthritis. To determine the roles of proinflammatory cytokines IL-1α, IL-1β, TNF-α, and IL-6 in the development of SKG arthritis, homozygously cytokine gene–deficient (–/–), heterozygously cytokine gene–deficient (+/–), or cytokine gene–intact (+/+) female SKG mice were prepared and maintained in our conventional animal facility, where the majority of cytokine gene–intact female SKG mice began to exhibit joint swelling at 11 to 12 weeks of age (Figure 3A). Severity of arthritis in these mice varied from swelling of some joints of the digits to marked swelling of large joints (the average score was 3.6 ± 1.5; see Methods for clinical assessment of arthritis) at 32 weeks of age. Histology of swollen joints of 32-week-old SKG mice revealed severe synovitis and destruction of cartilage and bone (Figure 3B). Notably, IL-6$^{-/-}$ SKG mice showed no joint swelling macroscopically, no histologically evident synovitis, and no destruction of cartilage and bone (Figure 3C). Some IL-1α/β$^{-/-}$ SKG mice started to develop arthritis around 15 weeks of age with a significantly lower incidence than IL-1α/β$^{+/+}$ SKG mice. Although the incidence in IL-1$^{-/-}$ mice was 60% at 32 weeks of age, severity was very low, with joint swelling restricted to only 1 or 2 joints of the digits. These swollen joints showed histologically evident synovitis but destruction of cartilage and bone was generally less severe than in cytokine-intact SKG mice (data not shown). These results were similar in the TNF-α$^{-/-}$ SKG mice: the onset was delayed, incidence lowered to 20% of control, and severity substantially reduced to swelling of a single joint of a digit (see legend to Figure 3A for statistical analyses of the data).

Interstitial pneumonitis — which was observed in SKG mice older than 8 months (12) — among these cytokine-deficient mice was too mild in severity and low in incidence at 32 weeks of age for comparisons to be made (data not shown).

IFN-γ–deficient SKG mice developed arthritis with no statistically significant differences in severity and incidence from IFN-γ$^{+/-}$ or IFN-γ$^{+/+}$ mice during 24 weeks of observation, although IFN-γ$^{-/-}$ SKG mice displayed progressive weight loss and died earlier as compared with wild-type controls maintained under the same conditions (12). We did not observe significant difference in histology between IFN-γ$^{-/-}$ and IFN-γ$^{+/-}$ or IFN-γ$^{+/+}$ mice, although the IFN-γ$^{-/-}$ mice, when they became debilitated, generally showed lesser degrees of arthritis compared with the IFN-γ$^{+/-}$ or IFN-γ$^{+/+}$ mice (data not shown). IL-4$^{-/-}$ SKG mice, on the other hand, survived well to 32 weeks of age; the time of onset, incidence and severity of arthritis were not significantly different among IL-4$^{-/-}$, IL-4$^{+/-}$, or IL-4$^{+/+}$ mice. Thus, IFN-γ and IL-4 are apparently dispensable for the development of SKG arthritis.

IL-10$^{-/-}$ SKG mice showed a consistently higher incidence of disease and mean arthritis score than IL-10$^{+/-}$ or IL-10$^{+/+}$ SKG mice, although the susceptibility to colitis of IL-10$^{-/-}$ mice restricted the period of observation to 24 weeks (15). Histological examination of IL-10$^{-/-}$ mice that had survived to this age showed severe synovitis accompanying joint destruction (Figure 3D). Thus, IL-10 is suppressive for the development of SKG arthritis.

In these experiments, SKG mice with heterozygous deficiency in IL-1, TNF-α, IL-6, or IL-10 showed incidences and severities of arthritis that were intermediate between those of homozygously cytokine-deficient and cytokine-intact mice. This result indicates that the disease-enhancing or -protective effects of the cytokines are dose dependent.

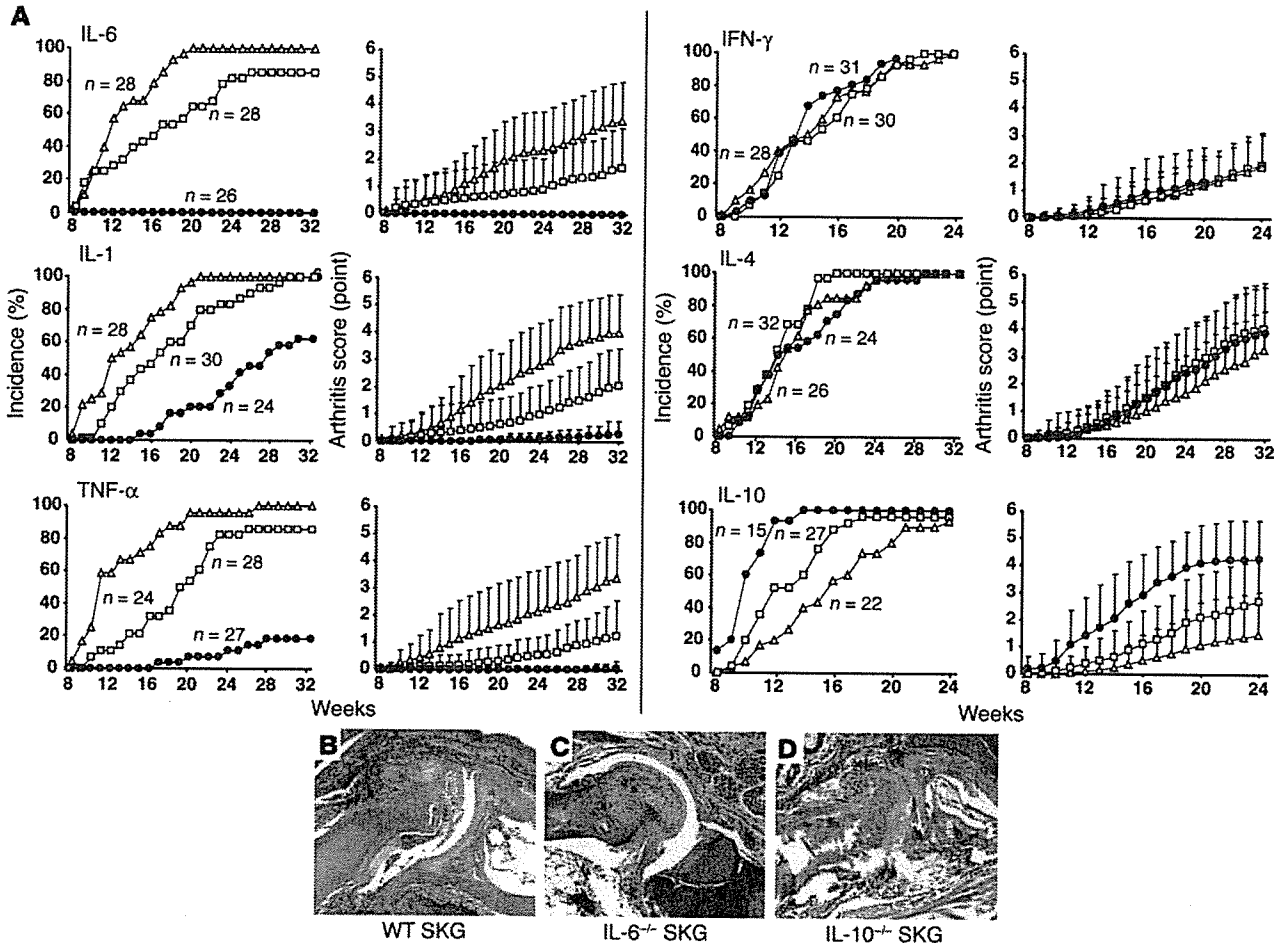

Figure 3
Development of arthritis in cytokine-deficient SKG mice. (**A**) Incidence and severity of arthritis in female SKG mice homozygously (–/–) (filled circles) or heterozygously (+/–) (open squares) deficient in indicated cytokines or cytokine-intact (+/+) (open triangles). Vertical bars represent the means ± SD of the whole group of mice. Arthritis scores are significantly different ($P < 0.01$) between IL-6$^{+/+}$ and IL-6$^{+/-}$ mice at 19–32 weeks; between IL-6$^{+/-}$ and IL-6$^{-/-}$ mice at 16–32 weeks; between IL-1$^{+/+}$ and IL-1$^{+/-}$ mice at 17–32 weeks; between IL-1$^{-/-}$ and IL-1$^{+/-}$ mice at 19–32 weeks; between TNF-α$^{+/+}$ and TNF-α$^{+/-}$ mice at 15–32 weeks; between TNF-α$^{-/-}$ and TNF-α$^{+/-}$ mice at 21–32 weeks; between IL-10$^{+/+}$ and IL-10$^{+/-}$ mice at 18–24 weeks; and between IL-10$^{-/-}$ and IL-10$^{+/-}$ mice at 12–24 weeks. (**B–D**) Histology of finger joints of a 32-week-old wild-type (**B**) or IL-6–deficient (**C**) or a 24-week-old IL-10–deficient SKG mouse (**D**) (original magnification, ×10).

RF and joint inflammation. The IL-6–, TNF-α–, or IL-1–deficient mice developed high titers of IgM-type RF even in the absence of joint inflammation (Figure 4A). This indicates that the development of IgM-RF is independent of joint inflammation. The result contrasted with the development of IgG anti-type II collagen autoantibody in arthritic mice but not in nonarthritic IL-6–deficient mice, which suggests the possible roles of anti-type II collagen antibody as an active mediator of joint inflammation or a product of joint destruction (Figure 4B).

Discussion

This study showed that proliferative synovitis with pannus formation and resultant joint destruction in SKG mice are immunopathologically similar to those observed in human RA and that, despite the pleiotropy, redundancy, and cross-regulation in cytokine functions, deficiency in either IL-6, IL-1, or TNF-α can inhibit the development and progression of SKG arthritis, which is apparently independent of the development of RF.

It is well documented in human RA and in animal models that IL-1, IL-6, and TNF-α synergistically mediate synovitis and destruction of cartilage and bone (1–3, 5, 6, 16–19), that IL-1 and TNF-α trigger the secretion of IL-6 by synovial cells (2), and that anti–TNF-α treatment can lower IL-6 formation (20, 21). It is still unclear, however, how the formation and action of these cytokines are controlled at molecular and cellular levels (22–24). Here we showed that IL-6 is apparently produced by subsynovial stromal cells (macrophages and DCs; Figure 1) and presumably some CD4$^+$ T cells, whereas IL-1 and TNF-α are mainly produced by superficial lining cells facing the joint cavity and producing matrix metalloproteinases as also shown in other arthritis models and RA (25–28). This difference in cellular sources between IL-6 and IL-1/TNF-α indicates that not only neutralization of these cytokines or blockade of their actions at a molecular level, but also reduction in the number of the stromal cells producing each cytokine or modifying their functions may ameliorate arthritis.

TNF-α deficiency inhibited arthritis effectively but not completely in SKG mice; i.e., the onset was delayed, incidence lowered

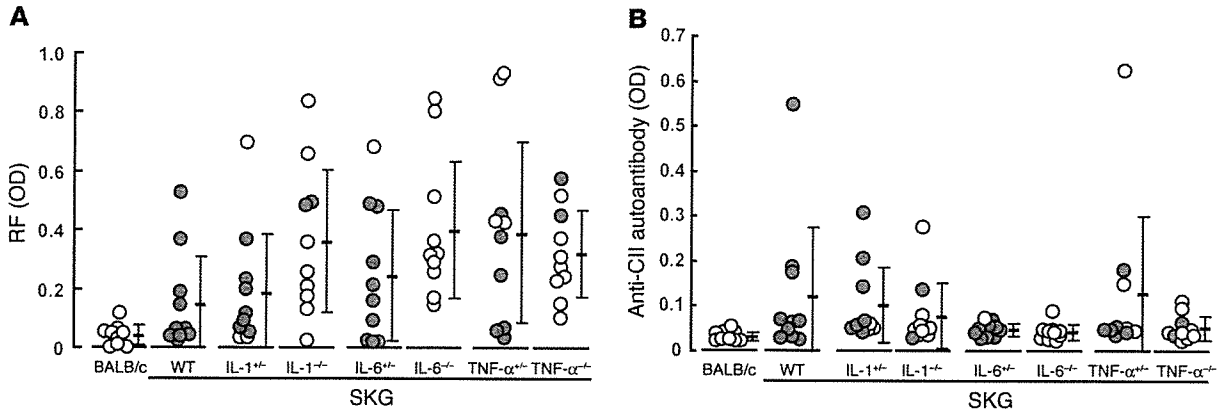

Figure 4

Autoantibodies in cytokine-deficient SKG mice. RF (**A**) or anti–type II collagen (anti-CII) autoantibody titers (**B**) in 32-week-old SKG mice homozygously or heterozygously deficient in indicated cytokines, with wild-type SKG mice and age-matched BALB/c mice as controls. Filled circles indicate mice with joint swelling (arthritis score ≥ 1.0); open circles indicate mice without joint swelling (arthritis score < 1.0). First 10 mice that had reached 32 weeks of age in each group shown in Figure 3 were analyzed.

to 20% of controls, and severity substantially reduced to swelling of a single joint of a digit. It can be argued that the MHC haplotype of TNF-α–deficient SKG mice could influence the development of arthritis, since TNF-α–deficient SKG mice bear an H-2b haplotype in contrast with SKG mice, which bear an H-2d haplotype. This is because the founder strain of TNF-α deficiency was of H-2b haplotype, and the TNF-α locus, which is closely linked with the MHC locus, was cosegregated with the MHC in establishing the congenic TNF-α–deficient SKG mice (29). We previously showed that the MHC haplotype of SKG mice can influence the incidence and severity of arthritis (e.g., H-2d haplotype confers susceptibility to arthritis in SKG mice [ref. 12]). It is unlikely, however, that the H-2b haplotype of TNF-α–deficient SKG mice alters the incidence and severity of arthritis, because SKG mice on BALB.B (H-2b) background showed an incidence and severity of arthritis similar to those of SKG mice (our unpublished data). Thus, TNF-α deficiency per se can inhibit the development of arthritis. On the other hand, the failure of TNF-α deficiency to completely inhibit arthritis suggests that proinflammatory cytokine pathways that spare TNF-α may also be operative in SKG arthritis. This substantial but incomplete inhibition of SKG arthritis by TNF-α deficiency may have a common basis with the clinical result that only about 30–40% of RA patients show dramatic responses to TNF inhibitors (30).

It is well documented in arthritis that pro- or anti-inflammatory cytokines facilitate or inhibit activation of various types of cells, including macrophages/monocytes, neutrophils, and T cells, which are involved in local inflammation (16). Another function of cytokines may be to alter the degree of T cell–mediated control of autoimmune T cells, thereby allowing arthritogenic T cells to chronically mediate arthritis. For example, IL-10 not only suppresses the formation of TNF-α and IL-6 by macrophages, synoviocytes, and T cells, as shown in other experimental models (31–33), but also may mediate or augment $CD25^+CD4^+$ T cell–mediated immunoregulation, as shown in other autoimmune/inflammatory diseases (34, 35). IL-10 deficiency may therefore attenuate the T cell–mediated suppression on arthritogenic T cells, thus contributing to the exacerbation of arthritis in SKG mice. Furthermore, in addition to its local and systemic proinflammatory effects (20, 36), IL-6 may render arthritogenic T cells refractory to the suppressive control exerted by naturally arising $CD25^+CD4^+$ regulatory T cells (37). $CD25^+CD4^+$ T cells, derived from normal BALB/c mice, indeed prevented SKG arthritis effectively when the animals were inoculated before onset of the disease, as observed in CIA (ref. 38 and our unpublished data). We are currently investigating whether IL-6 deficiency rectifies the susceptibility of arthritogenic T cells to the $CD25^+CD4^+$ T cell–mediated suppression and thereby contributes to inhibiting the development of SKG arthritis. Whether TNF-α or IL-1 can affect T cell–mediated immunoregulation by altering the functions of APCs or regulatory T cells also remains to be determined (39).

Although $CD4^+$ T cells play pivotal roles in SKG arthritis, they show impaired activation and proliferation upon T cell receptor stimulation because of a structurally altered ZAP-70 and resulting alteration in T cell signal transduction in SKG T cells (12). Despite this defect, SKG T cells are competent in secreting various cytokines, including IL-2, IL-4, IL-10, TNF-α, and IFN-γ, upon PMA/ionomycin stimulation, in a pattern of cytokine production and kinetics similar to that of BALB/c T cells (Supplemental Figure 5A). $CD4^+$ T cells from young SKG mice even produced slightly higher amounts of IFN-γ, IL-4, and IL-10 and smaller amounts of TNF-α than BALB/c $CD4^+$ T cells (Supplemental Figure 5B). Moreover, there was no significant alteration of the disease course in SKG mice with IFN-γ or IL-4 deficiency, which is in contrast with other models (40, 41). These findings taken together indicate that SKG $CD4^+$ T cells are not committed to Th1 or Th2 cells, or TNF-α production, due to the altered signal transduction through ZAP-70; skewing of $CD4^+$ arthritogenic T cells to either Th1 or Th2 is not absolutely required for the development and/or progression of arthritis; and cross-regulation, if any, by Th1 or Th2 cells is not significant in inhibiting arthritis in this model. It is possible that T cells in SKG mice trigger the activation and proliferation of synoviocytes in a cell-contact manner or via other cytokines (42). Notably, a large amount of mRNA for IL-17, which is secreted by activated T cells and able to stimulate synovial cells (43), can be detected in the joints of arthritic SKG mice (our unpublished data).

The disease in SKG mice is a chronic systemic inflammatory disease like human RA (1, 12). For example, SKG mice spontaneously develop RF as a systemic manifestation of the disease. An intriguing finding in cytokine-deficient SKG mice is that they developed high

titers of RF irrespective of whether arthritis was inhibited or not. For example, IL-6–deficient mice with no arthritis developed titers of RF equivalent to those of SKG mice. This cannot be attributed to hypergammaglobulinemia in SKG mice, because SKG mice without arthritis did not develop anti-DNA autoantibodies or anti–type II collagen autoantibodies, which may mediate joint inflammation or develop as a consequence of joint destruction (Figure 4) (12). Furthermore, transfer of thymocytes alone from SKG mice produced severe arthritis in SCID mice, which suggests that B cells may not be an absolute requirement for elicitation and progression of arthritis in this model (12). These results taken together indicate that RF is independent of joint inflammation per se in SKG mice. It is known, on the other hand, that RA patients with RF undergo a more aggressive and destructive course of arthritis (1). Considering that RF also develops in various other inflammatory diseases including microbial infections, it is likely that RF may not be a primary mediator of arthritis but may secondarily enhance joint inflammation, for example, by forming immune complexes that deposit in the joint (44, 45).

In conclusion, cytokines play essential roles in SKG arthritis in a manner similar to that in human RA. SKG mice can be instrumental for further studying the contribution of pro- and anti-inflammatory cytokines to the development and progression of RA, for elucidating how arthritogenic T cells stimulate synoviocytes to cause arthritis, and for devising effective treatment of the disease.

Methods

Mice. IL-1α/β–, TNF-α–, or IL-6–deficient mice (IL-1$^{-/-}$, TNF-α$^{-/-}$, and IL-6$^{-/-}$, respectively) were backcrossed to BALB/c mice more than 8 times (29). BALB/c IL-10–deficient (IL-10$^{-/-}$) mice were kindly provided by D. Rennick (DNAX Institute, Palo Alto, California, USA) (15). BALB/c IFN-γ$^{-/-}$ and IL-4$^{-/-}$ mice were purchased from The Jackson Laboratory (Bar Harbor, Maine, USA) (46, 47). These cytokine-deficient BALB/c mice were backcrossed three times to SKG mice, which have the BALB/c genetic background (12). Such *Skg*-homozygous but cytokine gene–heterozygous mice were intercrossed, and resulting female *Skg/Skg* littermates with homozygously or heterozygously cytokine-deficient or cytokine-intact female mice were used in the present study. All mice were maintained in our animal facility under conventional microbial conditions. All experiments were conducted according to the institutional guidelines for animal welfare of the Institute for Frontier Medical Sciences at Kyoto University.

Clinical assessment of SKG arthritis. Joint swelling was monitored by inspection and scored as follows: 0, no joint swelling; 0.1, swelling of one finger joint; 0.5, mild swelling of wrist or ankle; 1.0, severe swelling of wrist or ankle. Scores for all digits, wrists, and ankles were totaled for each mouse (12).

Antibodies. The following antibodies were used: anti-CD4 (H129.19), anti-CD8a (53-6.7), anti-CD11b (M1/70), anti-CD45RB/B220 (RA3-6B2), anti-CD49d (9C10), anti-CD106 (429), and anti-I-A/I-E (M5/114.15.2), purchased from BD Biosciences – Pharmingen (San Diego, California, USA); anti-IL-1β (AB-401-NA) (R&D Systems Inc., Minneapolis, Minnesota, USA); anti-TNF-α (L-19) (Santa Cruz Biotechnology Inc., Santa Cruz, California, USA); anti-IL-6 (D97) (Innogenetics, Gent, Belgium). For intracellular cytokine detection, the following mAb's were used: anti-IFN-γ (XMG1.2), anti-TNF-α (MP6-XT22), anti-IL-2 (JES6-5H4), anti-IL-4 (11B11), and anti-IL-10 (JES5-16E3) (BD Biosciences – Pharmingen).

RT-PCR. Total RNA was extracted from ankle joints using Isogen reagent (Nippon Gene Co., Tokyo, Japan) and reverse transcribed using Superscript II (Invitrogen Japan K.K., Tokyo, Japan). IL-1β, IL-6, or TNF-α mRNA levels were quantified by real-time PCR using QuantiTect Assay (Qiagen K.K., Tokyo, Japan) and normalized by hypoxanthine-guanin phosphoribosyl transferase (HPRT) as previously described (48). The quantities of these cytokine mRNAs were expressed as units by defining the levels of each cytokine mRNA in J774.1, a BALB/c macrophage cell line, stimulated with 1 μg/ml LPS for 24 hours, as one unit.

Histology and immunohistochemistry. Joints were fixed in 10% formalin, decalcified by 10% EDTA in PBS for 3 days, embedded in paraffin, sectioned, and stained with hematoxylin and eosin. For immunohistochemical staining, cryostat section of digits were fixed in cold acetone for 10 minutes, washed in PBS, and depleted of endogenous peroxidase by treatment with 0.3% H_2O_2 in absolute methanol for 15 minutes. After blocking nonspecific binding with 10% normal rabbit serum in PBS for 30 minutes, the sections were incubated with primary mAb's at appropriate dilutions for 1 hour at room temperature, washed, incubated with biotinylated rabbit anti-rat IgG pre-adsorbed with rabbit serum, washed and incubated with avidin-biotinylated horseradish peroxidase complex (ABC) and diaminobenzidine tetrahydrochloride (DAB) (Elite kit; Vector Laboratories Inc., Burlingame, California, USA), and counterstained with Mayer's hematoxylin.

For immunohistochemical staining of cytokines, sections were fixed for 15 minutes in ice-cold 4% phosphate-buffered paraformaldehyde (pH 7.4). The sections were then washed in HEPES-buffered saline solution (HEPES-BSS) (pH 7.1, Gibco; Invitrogen Corp., Carlsbad, California, USA) supplemented with 0.1% saponin (Sigma-Aldrich, St. Louis, Missouri, USA). All further incubations and washes were carried out using BSS-saponin. Endogenous peroxidase was inactivated by treatment with 1% formalin in BSS-saponin for 2 minutes, followed by sodium azide (0.1 M) containing 0.3% H_2O_2 for 30 minutes, blocked with 20% normal rabbit serum for 60 minutes, incubated overnight at 4°C with anti-cytokine mAb's at appropriate dilutions. The sections were then incubated with the secondary antibodies and ABC, as described above. Color was developed with AEC (DakoCytomation, Carpinteria, California, USA), and the sections were counterstained with Mayer's hematoxylin.

ELISA for autoantibody. Affinity-purified mouse IgG (5 μg/ml) and 10 μg/ml of bovine type II collagen (Funakoshi Co. Ltd., Tokyo, Japan) in PBS (pH 7.2) were used for overnight coating of ELISA plates (ICN Biomedicals Inc., Aurora, Ohio, USA). Test sera were diluted to 1:10 for anti–type II collagen antibody or 1:20 for RF assay. Alkaline phosphatase conjugated anti-mouse IgG or IgM (for RF assay) (Southern Biotechnology Associates Inc., Birmingham, Alabama, USA) was used at 1 μg/ml as the secondary reagent. Titer of RF and anti–type II collagen antibody was expressed as optical density (49).

ELISA for cytokines. The capsules of ankle joints were cut open, joint cavity was washed with 5 μl PBS, and 1 μl of withdrawn joint fluid was diluted 10-fold to assess the concentrations of IL-1β, IL-6, and TNF-α by ELISA (Biosource International, Camarillo, California, USA) according to the manufacturer's instruction, with the detection limits of 7 pg/ml for IL-1, 3 pg/ml for IL-6, and 3 pg/ml for TNF-α.

Statistics. Student's *t* test was used for statistical analyses.

Acknowledgments

This work was supported by grants-in-aid from the Ministry of Education, Science, Sports, and Culture, the Ministry of Human Welfare, and the Japan Science and Technology Agency. We thank Zoltan Fehervari for critical reading of the manuscript.

Received for publication April 5, 2004, and accepted in revised form June 29, 2004.

Address correspondence to: Shimon Sakaguchi, Department of Experimental Pathology, Institute for Frontier Medical Sciences, Kyoto University, 53 Shogoin Kawahara-cho, Sakyo-ku, Kyoto 606-8507, Japan. Phone: 81-75-751-3888; Fax: 81-75-751-3820; e-mail: shimon@frontier.kyoto-u.ac.jp.

1. Harris, E.D. 1997. *Rheumatoid arthritis.* W.B. Saunders. Philadelphia, Pennsylvania, USA. 417 pp.
2. Feldmann, M., Brennan, F.M., and Maini, R.N. 1996. Role of cytokines in rheumatoid arthritis. *Annu. Rev. Immunol.* **14**:397–440.
3. Choy, E.H., et al. 2002. Therapeutic benefit of blocking interleukin-6 activity with an anti-interleukin-6 receptor monoclonal antibody in rheumatoid arthritis: a randomized, double-blind, placebo-controlled, dose-escalation trial. *Arthritis Rheum.* **46**:3143–3150.
4. Elliott, M.J., et al. 1993. Treatment of rheumatoid arthritis with chimeric monoclonal antibodies to tumor necrosis factor alpha. *Arthritis Rheum.* **36**:1681–1690.
5. van de Loo, F.A., Kuiper, S., van Enckevort, F.H., Arntz, O.J., and van den Berg, W.B. 1997. Interleukin-6 reduces cartilage destruction during experimental arthritis. A study in interleukin-6-deficient mice. *Am. J. Pathol.* **151**:177–191.
6. Sasai, M., et al. 1999. Delayed onset and reduced severity of collagen-induced arthritis in interleukin-6-deficient mice. *Arthritis Rheum.* **42**:1635–1643.
7. Anguita, J., et al. 1998. Borrelia burgdorferi-infected, interleukin-6-deficient mice have decreased Th2 responses and increased lyme arthritis. *J. Infect. Dis.* **178**:1512–1515.
8. Alonzi, T., et al. 1998. Interleukin 6 is required for the development of collagen-induced arthritis. *J. Exp. Med.* **187**:461–468.
9. Ji, H., et al. 2002. Critical roles for interleukin 1 and tumor necrosis factor alpha in antibody-induced arthritis. *J. Exp. Med.* **196**:77–85.
10. Joosten, L.A., Helsen, M.M., van de Loo, F.A., and van den Berg, W.B. 1996. Anticytokine treatment of established type II collagen-induced arthritis in DBA/1 mice. A comparative study using anti-TNF alpha, anti-IL-1 alpha/beta, and IL-1Ra. *Arthritis Rheum.* **39**:797–809.
11. Takayanagi, H., et al. 2000. T-cell-mediated regulation of osteoclastogenesis by signalling cross-talk between RANKL and IFN-gamma. *Nature.* **408**:600–605.
12. Sakaguchi, N., et al. 2003. Altered thymic T-cell selection due to a mutation of the ZAP-70 gene causes autoimmune arthritis in mice. *Nature.* **426**:454–460.
13. Firestein, G.S., Yeo, M., and Zvaifler, N.J. 1995. Apoptosis in rheumatoid arthritis synovium. *J. Clin. Invest.* **96**:1631–1638.
14. van Dinther-Janssen, A.C., et al. 1991. The VLA-4/VCAM-1 pathway is involved in lymphocyte adhesion to endothelium in rheumatoid synovium. *J. Immunol.* **147**:4207–4210.
15. Kuhn, R., Lohler, J., Rennick, D., Rajewsky, K., and Muller, W. 1993. Interleukin-10-deficient mice develop chronic enterocolitis. *Cell.* **75**:263–274.
16. Arend, W.P. 2001. Physiology of cytokine pathways in rheumatoid arthritis. *Arthritis Care Res.* **45**:101–106.
17. Probert, L., Plows, D., Kontogeorgos, G., and Kollias, G. 1995. The type I interleukin-1 receptor acts in series with tumor necrosis factor (TNF) to induce arthritis in TNF-transgenic mice. *Eur. J. Immunol.* **25**:1794–1797.
18. Dayer, J.M., Beutler, B., and Cerami, A. 1985. Cachectin/tumor necrosis factor stimulates collagenase and prostaglandin E2 production by human synovial cells and dermal fibroblasts. *J. Exp. Med.* **162**:2163–2168.
19. Miyasaka, N., et al. 1988. Augmented interleukin-1 production and HLA-DR expression in the synovium of rheumatoid arthritis patients. Possible involvement in joint destruction. *Arthritis Rheum.* **31**:480–486.
20. Guerne, P.A., Zuraw, B.L., Vaughan, J.H., Carson, D.A., and Lotz, M. 1989. Synovium as a source of interleukin 6 in vitro. Contribution to local and systemic manifestations of arthritis. *J. Clin. Invest.* **83**:585–592.
21. Charles, P., et al. 1999. Regulation of cytokines, cytokine inhibitors, and acute-phase proteins following anti-TNF-alpha therapy in rheumatoid arthritis. *J. Immunol.* **163**:1521–1528.
22. Kishimoto, T., Taga, T., and Akira, A. 1994. Cytokine signal transduction. *Cell.***76**:253–262.
23. Lockslay, R.M., Killeen, N., and Leonardo, M.J. 2001. The TNF and TNF receptor superfamilies: integrating mammalian biology. *Cell.* **104**:487–501.
24. Firestein, G.S., and Manning, A.M. 1999. Signal transduction and transcription factors in rheumatic diseases. *Arthritis Rheum.* **42**:609–621.
25. Chu, C.Q., Field, M., Feldmann, M., and Maini, R.N. 1991. Localization of tumor necrosis factor alpha in synovial tissues and at the cartilage-pannus junction in patients with rheumatoid arthritis. *Arthritis Rheum.* **34**:1125–1132.
26. Ulfgren, A.K., Lindblad, S., Klareskog, L., Anderson, J., and Anderson, U. 1995. Detection of cytokine producing cells in the synovial membrane from patients with rheumatoid arthritis. *Ann. Rheum. Dis.* **54**:654–661.
27. Marinova-Mutafchieva, L., et al. 1997. Dynamics of proinflammatory cytokine expression in the joints of mice with collagen-induced arthritis (CIA). *Clin. Exp. Immunol.* **107**:507–512.
28. Okada, Y., Takeuchi, N., Tomita, K., Nakanishi, I., and Nagase, H. 1989. Immunolocalization of matrix metalloproteinase 3 (stromelysin) in rheumatoid synovioblasts (B cells): correlation with rheumatoid arthritis. *Ann. Rheum. Dis.* **48**:645–653.
29. Tanaka, J., et al. 2000. Lipopolysaccharide-induced HIV-1 expression in transgenic mice is mediated by tumor necrosis factor-alpha and interleukin-1, but not by interferon-gamma nor interleukin-6. *AIDS.* **14**:1299–1307.
30. Feldmann, M., and Maini, R.N. 2001. Anti-TNF alpha therapy of rheumatoid arthritis: what have we learned? *Annu. Rev. Immunol.* **19**:163–196.
31. Persson, S., Mikulowska, A., Narula, S., O'Garra, A., and Holmdahl, R. 1996. Interleukin-10 suppresses the development of collagen type II-induced arthritis and ameliorates sustained arthritis in rats. *Scand. J. Immunol.* **44**:607–614.
32. Walmsley, M., et al. 1996. Interleukin-10 inhibition of the progression of established collagen-induced arthritis. *Arthritis Rheum.* **39**:495–503.
33. Katsikis, P.D., Chu, C.Q., Brennan, F.M., Maini, R.N., and Feldmann, M. 1994. Immunoregulatory role of interleukin 10 in rheumatoid arthritis. *J. Exp. Med.* **179**:1517–1527.
34. Asseman, C., Mauze, S., Leach, M.W., Coffman, R.L., and Powrie, F. 1999. An essential role for interleukin 10 in the function of regulatory T cells that inhibit intestinal inflammation. *J. Exp. Med.* **190**:995–1004.
35. Goudy, K.S., et al. 2003. Systemic overexpression of IL-10 induces CD4$^+$CD25$^+$ cell populations in vivo and ameliorates type 1 diabetes in nonobese diabetic mice in a dose-dependent fashion. *J. Immunol.* **171**:2270–2278.
36. Naka, T., Nishimoto, N., and Kishimoto, T. 2002. The paradigm of IL-6: from basic science to medicine [review]. *Arthritis Res.* **4**(Suppl. 3):S233–S242.
37. Pasare, C., and Medzhitov, R. 2003. Toll pathway-dependent blockade of CD4$^+$CD25$^+$ T cell-mediated suppression by dendritic cells. *Science.* **299**:1033–1036.
38. Morgan, M.E., et al. 2003. CD25$^+$ cell depletion hastens the onset of severe disease in collagen-induced arthritis. *Arthritis Rheum.* **48**:1452–1460.
39. Wu, A.J., Hua, H., Munson, S.H., and McDevitt, H.O. 2002. Tumor necrosis factor-alpha regulation of CD4$^+$CD25$^+$ T cell levels in NOD mice. *Proc. Natl. Acad. Sci. U. S. A.* **99**:12287–12292.
40. Ortmann, R.A., and Shevach, E.M. 2001. Susceptibility to collagen-induced arthritis: cytokine-mediated regulation. *Clin. Immunol.* **98**:109–118.
41. Joosten, L.A., et al. 1997. Role of interleukin-4 and interleukin-10 in murine collagen-induced arthritis. Protective effect of interleukin-4 and interleukin-10 treatment on cartilage destruction. *Arthritis Rheum.* **40**:249–260.
42. Dayer, J.M., and Burger, D. 1999. Cytokines and direct cell contact in synovitis: relevance to therapeutic intervention. *Arthritis Res.* **1**:17–20.
43. Miossec, P. 2003. Interleukin-17 in rheumatoid arthritis: if T cells were to contribute to inflammation and destruction through synergy. *Arthritis Rheum.* **48**:594–601.
44. Roosnek, E., and Lanzavecchia, A. 1991. Efficient and selective presentation of antigen-antibody complexes by rheumatoid factor B cells. *J. Exp. Med.* **173**:487–489.
45. Mageed, R.A., Borretzen, M., Moyes, S.P., Thompson, K.M., and Natvig, J.B. 1997. Rheumatoid factor autoantibodies in health and disease. *Ann. N. Y. Acad. Sci.* **815**:296–311.
46. Dalton, D.K., et al. 1993. Multiple defects of immune cell function in mice with disrupted interferon-gamma genes. *Science.* **259**:1739–1745.
47. Noben-Trauth, N., Kohler, G., Burki, K., and Ledermann, B. 1996. Efficient targeting of the IL-4 gene in a BALB/c embryonic stem cell line. *Transgenic Res.* **5**:487–491.
48. Hori, S., Nomura, T., and Sakaguchi, S. 2003. Control of regulatory T cell development by the transcription factor Foxp3. *Science.* **299**:1057–1061.
49. Sakaguchi, S., and Sakaguchi, N. 1990. Thymus and autoimmunity: Capacity of the normal thymus to produce pathogenic self-reactive T cells and conditions required for their induction of autoimmune disease. *J. Exp. Med.* **172**:537–545.

TNF-α is crucial for the development of autoimmune arthritis in IL-1 receptor antagonist–deficient mice

Reiko Horai,[1,2] Akiko Nakajima,[1] Katsuyoshi Habiro,[3] Motoko Kotani,[3] Susumu Nakae,[1] Taizo Matsuki,[1] Aya Nambu,[1] Shinobu Saijo,[1] Hayato Kotaki,[1] Katsuko Sudo,[1] Akihiko Okahara,[4] Hidetoshi Tanioka,[4] Toshimi Ikuse,[4] Naoto Ishii,[5] Pamela L. Schwartzberg,[2] Ryo Abe,[3] and Yoichiro Iwakura[1]

[1]Center for Experimental Medicine, Institute of Medical Science, University of Tokyo, Tokyo, Japan. [2]National Human Genome Research Institute, NIH, Bethesda, Maryland, USA. [3]Research Institute for Biological Sciences, Tokyo University of Science, Chiba, Japan. [4]Santen Pharmaceutical Co., Osaka, Japan. [5]Department of Microbiology and Immunology, Tohoku University Graduate School of Medicine, Sendai, Japan.

IL-1 receptor antagonist–deficient (IL-1Ra$^{-/-}$) mice spontaneously develop autoimmune arthritis. We demonstrate here that T cells are required for the induction of arthritis; T cell–deficient IL-1Ra$^{-/-}$ mice did not develop arthritis, and transfer of IL-1Ra$^{-/-}$ T cells induced arthritis in *nu/nu* mice. Development of arthritis was also markedly suppressed by TNF-α deficiency. We found that TNF-α induced OX40 expression on T cells and blocking the interaction between either CD40 and its ligand or OX40 and its ligand suppressed development of arthritis. These findings suggest that IL-1 receptor antagonist deficiency in T cells disrupts homeostasis of the immune system and that TNF-α plays an important role in activating T cells through induction of OX40.

Introduction

RA is a systemic, chronic, inflammatory disorder exhibited most commonly in the joints. Although various factors including genetic factors, environmental factors, and infectious agents have been suggested as causes of the disease (1), so far the etiology and pathogenesis have not been completely elucidated. Patients often produce autoantibodies against various self components such as IgGs, type II collagen, and nuclear antigens, suggesting an autoimmune nature of the disease (2). Many proinflammatory cytokines, including IL-1 and TNF-α, chemokines, and growth factors, are expressed in diseased joints, forming a complex cytokine network. It is widely believed that dysregulation of the cytokine network contributes to the pathogenesis of RA (3).

IL-1 is a prototype proinflammatory cytokine and is produced by various types of cells, including monocytes/macrophages, lymphocytes, and synovial lining cells (4). Since IL-1 induces inflammation, promotes synovial cell growth, and promotes differentiation of osteoclasts, an important role for this cytokine in the development of RA has been suggested (1, 5). IL-1 receptor antagonist (IL-1Ra) is an endogenous inhibitor of IL-1. IL-1Ra production is induced by a number of other cytokines, viral products, and acute-phase proteins and is augmented in patients with autoimmune and inflammatory diseases, suggesting that IL-1Ra may play regulatory roles in these diseases (6). TNF-α is also thought to be importantly involved in the inflammation and bone destruction in RA. TNF-α is produced mainly by monocytes/macrophages, which are activated by soluble components of bacteria and by direct contact with activated T cells at inflammatory sites. The production of IL-1 is coordinated with that of TNF-α, and they mutually stimulate each other's production. Overproduction of these cytokines by gene manipulation has been found to predispose the organism to inflammatory arthritis (7–10).

Cumulative evidence suggests that T cell–mediated autoimmune responses play a crucial role in the pathogenesis of RA. In fact, it has been demonstrated that T cells from RA patients can cause inflammatory arthritis in SCID mice (11). T cells that invade tissues and cause autoimmune destruction express activation antigens that are not expressed on normal resting T cells. These activation antigens include the IL-2 receptor α (CD25), CD69, CD44, CD40 ligand (CD40L; also known as CD154), and OX40 (also known as CD134) (12) CD40L on T cells and its receptor on APCs, as well as OX40 on T cells and its ligand (OX40L) on APCs, generate costimulatory signals that enhance T cell proliferation and cytokine production. Indeed, the expression of OX40 on T cells in rheumatoid synovial tissues is quite pronounced in some patients (12), and blocking either CD40L or OX40L in vivo reduces the severity of collagen-induced arthritis (CIA), experimental allergic encephalomyelitis, and inflammatory bowel disease in animal models of these diseases (13, 14). However, the molecular mechanisms for the induction of these costimulatory molecules in RA are not fully understood. We previously reported that IL-1 plays an important role in enhancing T cell–APC interactions through induction of CD40L and OX40 on T cells (15). Thus, excess IL-1 signaling may activate these pathways, leading to the development of T cell–mediated autoimmune diseases.

We previously reported that IL-1Ra$^{-/-}$ mice on the BALB/c background spontaneously develop chronic inflammatory arthropathy (9). Histopathology showed marked synovial and periarticular inflammation, with articular erosion caused by invasion of granulation tissues closely resembling that of RA in humans. Moreover, elevated levels of antibodies against immunoglobulins (rheumatoid factor [RF]), type II collagen, and double-stranded DNA were detected in sera of these mice, consistent with the development

Nonstandard abbreviations used: CD40L, CD40 ligand; CIA, collagen-induced arthritis; IL-1Ra, IL-1 receptor antagonist; PEC, peritoneal exudate cells; RF, rheumatoid factor.

Conflict of interest: The authors have declared that no conflict of interest exists.

Citation for this article: *J. Clin. Invest.* 114:1603–1611 (2004). doi:10.1172/JCI200420742.

Table 1
Incidence of arthritis in IL-1Ra$^{-/-}$ *scid/scid* mice

Genotype of *scid* loci	Incidence (%)
scid/scid	0/6 (0%)[A]
scid/+	9/11 (82%)
+/+	7/8 (88%)

Incidence of arthritis was judged at 20 weeks of age. Development of arthritis was completely suppressed in T cell–deficient IL-1Ra$^{-/-}$ *scid/scid* mice. [A]$P < 0.01$ by chi-square for independence test.

of autoimmunity. Proinflammatory cytokines such as IL-1β, IL-6, and TNF-α were overexpressed in the joints, indicating regulatory roles of IL-1Ra in the cytokine network. These data therefore suggested that IL-1Ra is crucial for the homeostasis of the immune system. It is not known, however, which cells in the immune system are crucial for the regulation of IL-1 and its actions, or furthermore, which cytokines are involved in the pathogenesis of arthritis in this model.

In this study, to elucidate the pathogenesis of the autoimmune arthritis in IL-1Ra$^{-/-}$ mice, we assessed the role of T cells in the development of arthritis by transferring T cells from IL-1Ra$^{-/-}$ mice to *nu/nu* mice and by intercrossing IL-1Ra$^{-/-}$ mice with T cell–deficient mice. We show that IL-1Ra$^{-/-}$ deficiency in T cells is enough for the development of arthritis. Furthermore, we analyzed the role of TNF-α in this model by producing TNF-α$^{-/-}$ IL-1Ra$^{-/-}$ mice, and we were able to demonstrate that TNF-α is crucial for the development of arthritis, as it induces OX40 on T cells. Treatment with anti-CD40L or anti-OX40L Ab suppressed disease, demonstrating the importance of CD40-CD40L and OX40-OX40L interactions for the development of autoimmune arthritis.

Results

Development of arthritis is suppressed in T cell– and B cell–deficient IL-1Ra$^{-/-}$ mice. IL-1Ra$^{-/-}$ mice on the BALB/c background spontaneously developed chronic inflammatory arthritis. Since high levels of RF, antibody to type II collagen, and antibody to double-stranded DNA are observed in IL-1Ra$^{-/-}$ mice, we hypothesized that there could be an autoimmune mechanism for the pathogenesis. To address this question, we evaluated the contribution of T cells and/or B cells to the development of arthritis in IL-1Ra$^{-/-}$ mice by intercrossing them with *scid/scid* mice on the BALB/c background. While IL-1Ra$^{-/-}$ *scid/+* or IL-1Ra$^{-/-}$ *+/+* mice showed a high incidence of arthritis, IL-1Ra$^{-/-}$ *scid/scid* mice failed to develop arthritis by 20 weeks of age (Table 1). These results suggest that combined deficiency of T and B cells completely suppresses the development of arthritis in IL-1Ra$^{-/-}$ mice.

Peripheral T cells from IL-1Ra$^{-/-}$ mice induced arthritis. We next examined the contribution of the specific cell types of the immune system to the development of arthritis by cell transfer experiments. When total splenocytes from IL-1Ra$^{-/-}$ mice were transferred into *nu/nu* mice on the BALB/c background, these mice developed severe arthritis as early as 3 weeks after the cell transfer (Figure 1, A and B). On the other hand, when T cell–depleted splenocytes were transferred into *nu/nu* mice, these mice did not develop arthritis at all. These results strongly suggest that T cells are involved in the development of arthritis. We further examined the effects of transplantation of purified T cells in the periphery. When T cells from spleens and LNs were transferred into *nu/nu* mice, they developed severe arthritis as early as 2 weeks after transfer (Figure 1, C and D). The disease status of the donor mice influenced these results; T cells from arthritic mice were more efficient than those

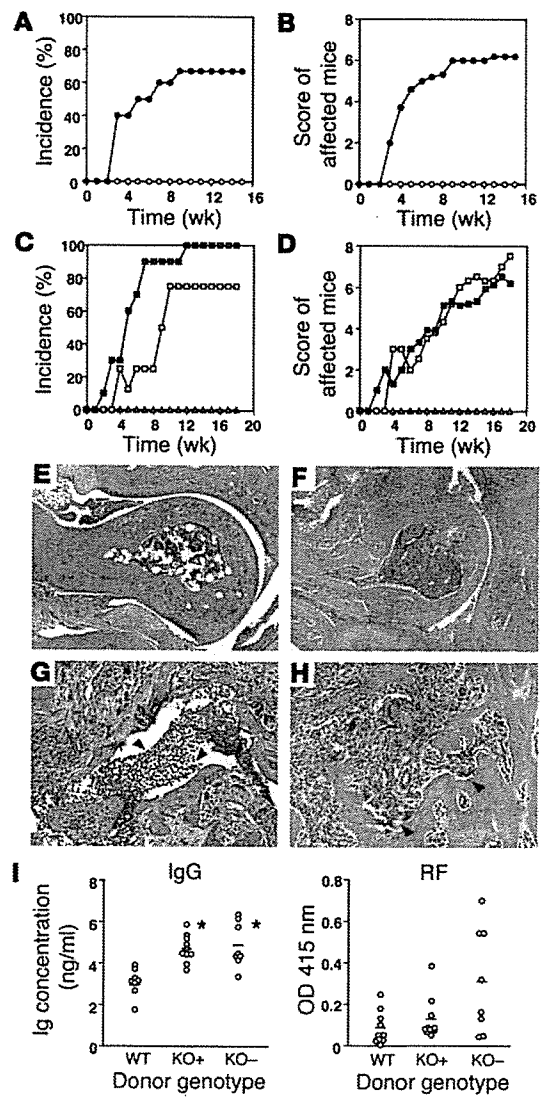

Figure 1
Splenocyte and T cell transfer into *nu/nu* mice. (**A**) Total splenocytes from IL-1Ra$^{-/-}$ mice (filled circles, $n = 10$) induced arthritis, while T cell–depleted splenocytes (open circles, $n = 7$) did not induce arthritis in *nu/nu* mice. (**B**) Arthritic severity score of splenocyte-transferred mice. (**C**) Purified T cells from spleen and LNs of either arthritic (filled squares, $n = 10$) or nonarthritic (open squares, $n = 8$) IL-1Ra$^{-/-}$ mice induced arthritis in *nu/nu* mice, while T cells from WT mice (triangles, $n = 11$) did not. (**D**) Arthritic severity score of T cell–transferred mice. (**E–H**) Histology of the ankle joints of WT (**E**) or IL-1Ra$^{-/-}$ (**F–H**) T cell–transferred *nu/nu* mice. (**G**) Infiltration of inflammatory cells (indicated by arrowheads). (**H**) Erosive bone destruction by replacement of bone matrix with fibroblastic cells (indicated by arrowheads). Magnification, ×40 (**E** and **F**); ×100 (**G** and **H**). (**I**) Serum IgG (left) and RF (right) levels in WT T cell– or IL-1Ra$^{-/-}$ T cell–transferred *nu/nu* mice. The average in each group is shown as a horizontal bar. WT, WT donors ($n = 10$); KO+, arthritic-IL-1Ra$^{-/-}$ donors ($n = 10$); KO–, nonarthritic IL-1Ra$^{-/-}$ donors ($n = 8$). *$P < 0.05$.

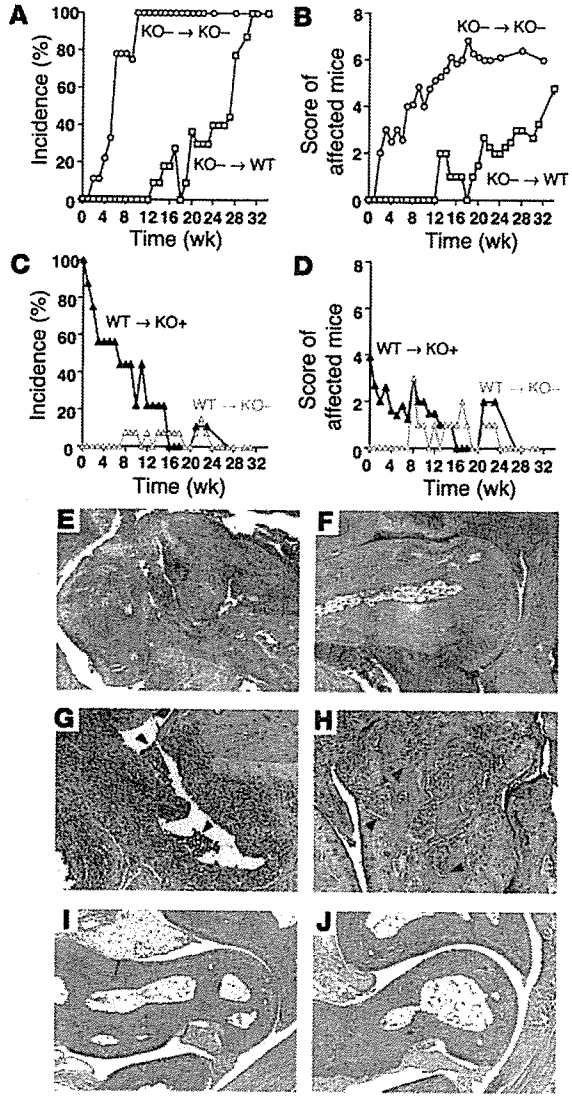

Figure 2
BM cell replacement between WT and IL-1Ra$^{-/-}$ mice. BM cells from IL-1Ra$^{-/-}$ mice induced arthritis in WT mice, while those from WT mice suppressed arthritis in IL-1Ra$^{-/-}$ mice. (**A**) Incidence of arthritis in IL-1Ra$^{-/-}$ BM cell–transferred WT (squares, $n = 11$) or IL-1Ra$^{-/-}$ mice (circles, $n = 9$). (**B**) Arthritic severity score of IL-1Ra$^{-/-}$ BM cell–transferred mice. (**C**) Incidence of arthritis in WT BM cell–transferred IL-1Ra$^{-/-}$ mice with (closed triangle, $n = 9$) or without (open triangle, $n = 13$) arthritis. (**D**) Arthritic severity score of WT BM–transferred IL-1Ra$^{-/-}$ mice. (**E–H**) Histopathology of the ankle joints of IL-1Ra$^{-/-}$ BM cell–transferred IL-1Ra$^{-/-}$ mice (**E**) and IL-1Ra$^{-/-}$ BM cell–transferred WT mice (**F–H**) at the end of the experiments (32 weeks and 34 weeks after the cell transfer, respectively). (**G**) Infiltration of inflammatory cells (indicated by arrowheads) into articular space and proliferation of the lining cells of the synovial membrane. (**H**) Pannus formation and erosive destruction of the bone (indicated by arrowheads). (**I** and **J**) Histology of the normal ankle joints of WT BM cell–transferred nonarthritic IL-1Ra$^{-/-}$ mice (**I**) and arthritic IL-1Ra$^{-/-}$ mice (**J**) at 31 weeks after the cell transfer. Magnification, ×40 (**E**, **F**, **I**, and **J**); ×100 (**G** and **H**).

from nonarthritic mice in inducing arthritis in recipient mice (Figure 1C). However, cells from both arthritic and nonarthritic mice could induce the disease. Histological analyses revealed that arthritis was observed in both ankle and knee joints of IL-1Ra$^{-/-}$ T cell–transferred *nu/nu* mice (Figure 1, F–H and data not shown). Proliferation of synovial cells, infiltration of neutrophils and lymphocytes, and bone destruction were remarkable in both ankle and knee joints (Figure 1, E–H and data not shown). Serum IgG levels and RF levels were enhanced in IL-1Ra$^{-/-}$ T cell–transferred *nu/nu* mice compared with WT T cell–transferred mice, although the difference in RF levels was not statistically significant (Figure 1I). We also performed thymocyte transfer experiments to examine whether or not activation of IL-1Ra$^{-/-}$ T cells before transplantation is necessary, and we found that thymocytes from IL-1Ra$^{-/-}$ mice induced arthritis in *nu/nu* mice, but with lower frequency than that seen in mice transferred with splenocytes or purified T cells (IL-1Ra$^{-/-}$ thymocyte–transferred mice, 46%; WT thymocyte–transferred mice, 0% at 15 weeks). These results clearly indicate that T cells are required for the development of arthritis in IL-1Ra$^{-/-}$ mice, and suggest that IL-1Ra$^{-/-}$ T cells can enhance immune responses against self components.

BM-derived cells from IL-1Ra$^{-/-}$ mice induced arthritis in normal mice and those from normal mice suppressed the development of arthritis in IL-1Ra$^{-/-}$ mice. To examine whether abnormal T cell education or a stem cell disorder is responsible for the T cell abnormality seen in IL-1Ra$^{-/-}$ mice, we next reconstituted the immune system by BM cell transfers. BM cells were prepared from IL-1Ra$^{-/-}$ mice by treating these cells with anti-Thy-1.2 Ab to deplete T cells, and then they were transferred into the recipient mice that were lethally irradiated. Mice that received BM cells did not die, whereas those that did not receive BM cells died within 2 weeks. We observed the development of arthritis as early as 2 weeks after the transfer of 4-week-old IL-1Ra$^{-/-}$ BM cells to nonarthritic IL-1Ra$^{-/-}$ mice, which would normally develop arthritis at 5–8 weeks of age (Figure 2A). Arthritis was also observed in WT mice receiving IL-1Ra$^{-/-}$ BM cells. These mice developed arthritis, however, more than 3 months after the transfer, indicating that the genotype of recipient mice (WT or IL-1Ra–deficient) affects the incidence and severity of arthritis (Figure 2, A and B). Replacement of the recipient BM cells by the donor cells was confirmed by Southern blot analyses at the end of the experiments. Cells from lymphoid tissues such as the spleen and LNs consisted mainly of the donor cells, while those from joints showed both donor and recipient genotypes (data not shown), suggesting that only BM-derived cells were replaced in the joints (16). Histological analysis of the ankle joints showed synovial and periarticular inflammation with articular erosion in both WT and IL-1Ra$^{-/-}$ mice that received IL-1Ra$^{-/-}$ BM cells (Figure 2, E and F). We observed proliferation of synovial lining cells and invasion of inflammatory cells, includ-

Table 2
Increased cytokine secretion by CD4$^+$ T cells from IL-1Ra$^{-/-}$ mice

Cytokine	Detection limit	WT	IL-1Ra$^{-/-}$
IFN-γ (U/ml)	20 U/ml	59.7 ± 13.0	153.8 ± 19.1^A
IL-4 (pg/ml)	10 pg/ml	42.0 ± 5.0	161.9 ± 3.2^A
TNF-α (pg/ml)	12.5 pg/ml	52.0 ± 7.8	95.3 ± 3.7^A

Purified CD4$^+$ T cells were stimulated with 1 μg/ml (IFN-γ and IL-4) or 10 μg/ml (TNF-α) of plate-coated anti-CD3 mAb for 48 hours. Data are expressed as mean ± SEM ($n = 4$). $^AP < 0.01$ by Student's t test. Similar results were obtained from 2 independent experiments.

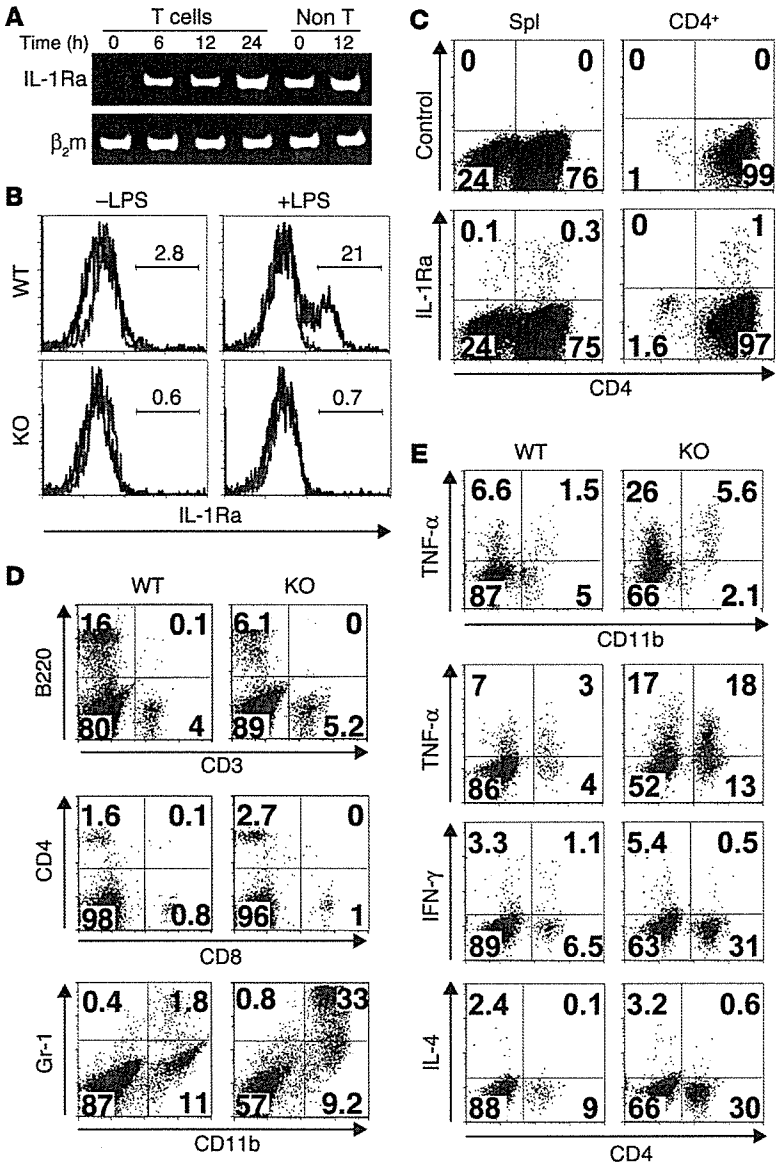

Figure 3
IL-1Ra and cytokine production. (**A**) *IL-1Ra* mRNA expression in WT T cells. Purified T cells from WT mice were stimulated with 10 μg/ml of plate-coated anti-CD3 mAb for 0, 6, 12, or 24 hours, and *IL-1Ra* mRNA levels were determined by RT-PCR. T cell–depleted splenocytes (Non T) were stimulated with 5 μg/ml LPS for 0 and 12 hours as controls. β_2m is used as an internal control. (**B**) Intracellular staining for IL-1Ra in PECs. PECs from WT and IL-1Ra$^{-/-}$ mice were stimulated with LPS, and IL-1Ra$^+$ cells in the CD11b$^+$ population are shown as histograms. Black-lined histograms: staining with IL-1Ra Ab. Gray-lined histograms: staining with isotype control Ig. Percentages of IL-1Ra$^+$ cells are indicated. (**C**) Intracellular staining for IL-1Ra in splenocytes (Spl) and CD4$^+$ T cells from WT mice after stimulation with anti-CD3 mAb. Upper panels show staining with isotype control Ig and lower panels show staining with anti–IL-1Ra Ab. (**D**) Expression of cell lineage–specific surface molecules on cells from ankle joints of WT and IL-1Ra$^{-/-}$ (KO) mice. B220, Gr-1, and CD11b are markers for B cells, granulocytes (including neutrophils), and macrophages, respectively. (**E**) Intracellular staining for cytokines in cells from the ankle joints of WT and IL-1Ra$^{-/-}$ mice. Joint-derived cells were stimulated with 10 ng/ml PMA and 400 ng/ml ionomycin for 6 hours with 2 μM monensin. Similar results were obtained in 3 independent experiments.

ing lymphocytes and neutrophils (Figure 2, E–G). Bone erosion and pannus formation were also remarkable (Figure 2H).

To examine whether normal stem cells can suppress the development of arthritis in IL-1Ra$^{-/-}$ mice, we prepared BM cells from WT mice and transferred them into irradiated nonarthritic or arthritic IL-1Ra$^{-/-}$ mice. Development of arthritis was suppressed in nonarthritic IL-1Ra$^{-/-}$ mice that received normal BM cells (Figure 2, C and D). Arthritis was also ameliorated in arthritic IL-1Ra$^{-/-}$ mice that received normal BM cells (Figure 2, C and D). At 31 weeks after transfer of BM cells, joint pathology was examined histologically. Nonarthritic IL-1Ra$^{-/-}$ mice that received normal BM cells showed no sign of arthritis (Figure 2I). Moreover, arthritic IL-1Ra$^{-/-}$ mice that received normal BM cells showed complete recovery from arthritis (Figure 2J). Thus, replacement of the BM-derived cells in IL-1Ra$^{-/-}$ mice with those of normal mice can suppress and actually reverse the development of arthritis in IL-1Ra$^{-/-}$ mice. These results indicate that BM-derived cells themselves are abnormal in IL-1Ra$^{-/-}$ mice.

Enhanced cytokine production from activated T cells in IL-1Ra$^{-/-}$ mice. Since our results suggested abnormal T cell function in IL-1Ra$^{-/-}$ mice, we next analyzed T cell proliferation and cytokine production upon TCR stimulation. Proliferative responses of T cells from IL-1Ra$^{-/-}$ mice stimulated with anti-CD3 mAb were normal (data not shown). However, these T cells produced much higher levels of IFN-γ, IL-4, and TNF-α in the culture supernatant than did those from WT mice (Table 2). These results suggest that IL-1Ra$^{-/-}$ T cells produce higher levels of cytokines upon TCR stimulation.

We also examined IL-1Ra expression in normal WT T cells by RT-PCR, ELISA, and intracellular staining. Unstimulated T cells expressed low levels of *IL-1Ra* mRNA, but upon stimulation through TCR, *IL-1Ra* mRNA expression was upregulated (Figure 3A). We also observed secretion of the IL-1Ra protein in the culture supernatant of WT purified CD4$^+$ T cells (>99% purity) after anti-CD3 mAb stimulation (20–40 pg/ml at 72–96 hours), indicating that T cells can produce and secrete the IL-1Ra protein. To confirm the IL-1Ra protein production from T cells directly, we stained stimulated CD4$^+$ T cells intracellularly with anti–IL-1Ra Ab. As a control experiment for the staining, we first stained peritoneal exudate cells (PECs) from WT or IL-1Ra$^{-/-}$ mice stimulated with or without LPS, and showed that the staining specifically detected IL-1Ra after the stimulation (Figure 3B). Then, purified CD4$^+$ T cells from BALB/c WT mice were stimulated with plate-coated anti-CD3 mAb and stained for the intracellular IL-1Ra protein. As shown in Figure 3C, CD4$^+$ T cells can produce IL-1Ra protein after TCR stimulation. These IL-1Ra–producing cells were different from those which produce IFN-γ, IL-4, or IL-10 under these conditions (data not shown). These results indicate that IL-1Ra is produced by T cells and may regulate T cell activation by IL-1.

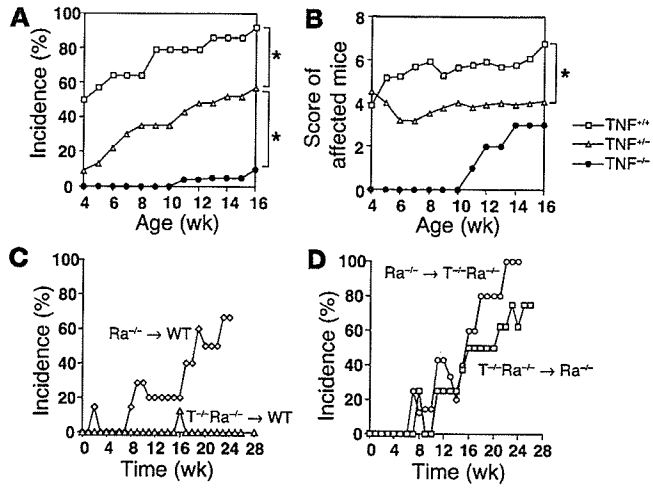

Figure 4
Incidence of arthritis in TNF-α–deficient IL-1Ra$^{-/-}$ mice. Incidence (**A**) and severity score (**B**) of arthritis in TNF-α–deficient IL-1Ra$^{-/-}$ mice. Squares, TNF-α$^{+/+}$ IL-1Ra$^{-/-}$ mice (n = 14); triangles, TNF-α$^{+/-}$ IL-1Ra$^{-/-}$ mice (n = 23); circles, TNF-α$^{-/-}$ IL-1Ra$^{-/-}$ mice (n = 23). Statistical significance between genotypes was calculated by repeated-measures ANOVA or two-way ANOVA. *P < 0.01. (**C**) Incidence of arthritis in TNF-α$^{-/-}$ IL-1Ra$^{-/-}$ (Ra$^{-/-}$) or IL-1Ra$^{-/-}$ BM cell–transferred WT mice. Triangles, WT mice transferred with TNF-α$^{-/-}$ IL-1Ra$^{-/-}$ BM cells (T$^{-/-}$Ra$^{-/-}$ → WT); diamonds, WT or heterozygous (IL-1Ra$^{+/-}$) mice transferred with IL-1Ra$^{-/-}$ BM cells (Ra$^{-/-}$ → WT). (**D**) Incidence of arthritis in TNF-α$^{-/-}$ IL-1Ra$^{-/-}$ or IL-1Ra$^{-/-}$ BM cell–transferred IL-1Ra$^{-/-}$ mice. Squares, IL-1Ra$^{-/-}$ mice transferred with TNF-α$^{-/-}$ IL-1Ra$^{-/-}$ BM cells (T$^{-/-}$Ra$^{-/-}$ → Ra$^{-/-}$); circles, TNF-α$^{-/-}$ IL-1Ra$^{-/-}$ mice transferred with IL-1Ra$^{-/-}$ BM cells (Ra$^{-/-}$ → T$^{-/-}$Ra$^{-/-}$).

Identification of cells in the joints and cellular cytokine production. To further analyze the roles of cytokines overexpressed in IL-1Ra$^{-/-}$ T cells, we examined the local subsets of lymphocytes and their cytokine production in the joints. The ankle joints were dissected, and cytokine production in the joint cells was examined by intracellular staining. The total cell number in the ankle joints was increased 2-fold in IL-1Ra$^{-/-}$ mice (7.1 × 10^6 cells per mouse, n = 10) compared to WT mice (3.7 × 10^6 cells per mouse, n = 10), suggesting infiltration of inflammatory cells. Thus, although the proportion of T cells was not dramatically increased (Figure 3D), the total T cell numbers in the joints of IL-1Ra$^{-/-}$ mice were greater than in WT mice. In the T lymphocyte subsets, CD4$^+$ cells were detected more frequently than CD8$^+$ cells, consistent with our previous observations (17). We also observed increased infiltration of CD11b$^+$ Gr-1$^+$ cells, most likely activated neutrophils, in the arthritic joints of IL-1Ra$^{-/-}$ mice (Figure 3D).

Cells from the ankle joints were stimulated with PMA and ionomycin to examine the ability to produce cytokines such as TNF-α, IFN-γ, and IL-4. As shown in Figure 3E, most of the IL-1Ra$^{-/-}$ CD11b$^+$ cells produced TNF-α. Some of CD4$^+$ T cells in the joints were also TNF-α–producing cells. Moreover, many more of these cells were found in the IL-1Ra$^{-/-}$ joints, suggesting that the infiltrating CD4$^+$ T cells in arthritic joints may produce more TNF-α and enhance inflammation. Only a small percentage of cells in the joints produced IFN-γ or IL-4 in either WT mice or IL-1Ra$^{-/-}$ mice.

Suppression of arthritis in TNF-α–deficient IL-1Ra$^{-/-}$ mice. We previously reported that high levels of inflammatory cytokines, including TNF-α, were detected in the joints of IL-1Ra$^{-/-}$ mice (9). We also observed TNF-α–producing cells in the ankle joints of these mice (Figure 3E). Furthermore, we detected high levels of TNF-α in the culture of IL-1Ra$^{-/-}$ T cells (Table 2). To elucidate the role of TNF-α in the development of arthritis in IL-1Ra$^{-/-}$ mice, we generated TNF-α and IL-1Ra double-deficient mice by crossing IL-1Ra$^{-/-}$ mice with TNF-α$^{-/-}$ mice.

As shown in Figure 4, A and B, homozygous TNF-α deficiency strongly suppressed development of arthritis in IL-1Ra$^{-/-}$ mice. An intermediate, but significant, suppression was observed in mice heterozygous for the *TNF*-α gene, suggesting a *TNF*-α gene dosage effect on the incidence and severity of arthritis. Histological analyses revealed that TNF-α$^{-/-}$ IL-1Ra$^{-/-}$ mice that appeared normal also showed normal joint histology, but those with swollen joints showed arthritic pathology of inflammation and bone destruction similar to that seen in IL-1Ra$^{-/-}$ mice (data not shown). These results suggest that TNF-α plays critical roles in the development of arthritis in IL-1Ra$^{-/-}$ mice.

However, since the *TNF*-α gene is located in the MHC locus and mice deficient for this gene were produced on the 129 background (H-2^b), TNF-α$^{-/-}$ mice backcrossed to the BALB/c strain (H-2^d) for 8 generations still had the same H-2 locus as the 129 mice. To examine the contribution of the MHC locus in the development of arthritis in IL-1Ra$^{-/-}$ mice, IL-1Ra$^{-/-}$ mice were crossed with the BALB.B congenic for the C57BL/6 H-2 locus (H-2^b) or the B10.D2/n congenic for the BALB/c H-2 locus. The results clearly argued that MHC differences were not responsible for the suppression of arthritis in TNF-α$^{-/-}$ mice (data not shown).

To further analyze the role of TNF-α in the development of arthritis in IL-1Ra$^{-/-}$ mice, we examined the effects of TNF-α deficiency in BM cell transfer experiments. BM cells from TNF-α$^{-/-}$ IL-1Ra$^{-/-}$ mice did not induce arthritis in WT mice up to 30 weeks after transfer, while BM cells from IL-1Ra$^{-/-}$ mice induced arthritis in WT mice starting after 8 to 12 weeks (Figures 2A and 4C). On the other hand, TNF-α$^{-/-}$ IL-1Ra$^{-/-}$ BM cells transferred into IL-1Ra$^{-/-}$ mice induced arthritis, and IL-1Ra$^{-/-}$ BM cells transferred into TNF-α$^{-/-}$ IL-1Ra$^{-/-}$ mice also induced arthritis (Figure 4, C and D). These results suggest that TNF-α produced by both BM-derived cells and non-BM-derived cells plays an important role in the development of arthritis

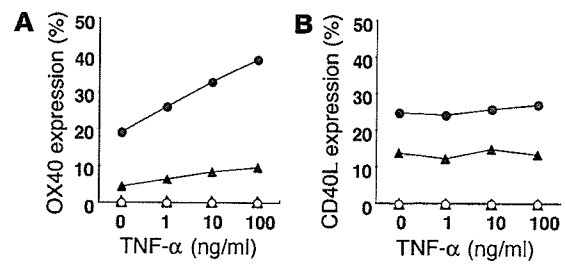

Figure 5
Induction of OX40 expression on T cells by TNF-α. (**A**) OX40 expression (%) on CD4$^+$ T cells stimulated with plate-coated anti-CD3 mAb (0.1 or 0.3 μg/ml) plus TNF-α (0, 1, 10, or 100 ng/ml) for 72 hours. Open symbols: control Ig staining. Filled symbols: anti-OX40 Ab staining for 0.1 μg/ml (triangles) or 0.3 μg/ml (circles) of anti-CD3 mAb stimulation. (**B**) CD40L expression (%) on CD4$^+$ T cells stimulated with plate-coated anti-CD3 mAb (0.1 or 0.3 μg/ml) plus TNF-α (0, 1, 10, or 100 ng/ml) for 24 hours. Open symbols: control Ig staining. Filled symbols: anti-OX40 Ab staining for 0.1 μg/ml (triangles) or 0.3 μg/ml (circles) of anti-CD3 mAb stimulation. Similar results were obtained in 2 to 5 independent experiments.

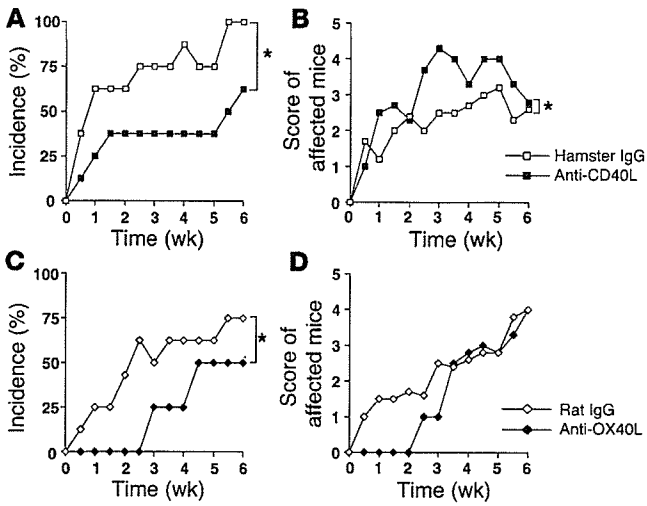

Figure 6

Anti-CD40L or anti-OX40L Ab treatment of IL-1Ra$^{-/-}$ mice. Blocking Abs against either CD40L or OX40L were administrated to IL-1Ra$^{-/-}$ mice before the onset of arthritis. Ab treatment was continued twice a week for 6 weeks, and incidence of arthritis was inspected each time before Ab administration. Incidence and severity score of arthritis in control hamster IgG–treated (open squares, $n = 8$) or anti-CD40L Ab–treated (filled squares, $n = 8$) IL-1Ra$^{-/-}$ mice (**A** and **B**) and those in control rat IgG–treated (open diamonds, $n = 8$) or anti-OX40L Ab–treated (closed diamonds, $n = 8$) IL-1Ra$^{-/-}$ mice (**C** and **D**). *$P < 0.01$ by repeated-measures ANOVA or 2-way ANOVA.

in IL-1Ra$^{-/-}$ mice. Since TNF-α is crucial for the development of arthritis in this model, these results suggest that TNF-α can be produced in the IL-1Ra$^{-/-}$ recipient mice from relatively γ-ray–resistant cells such as macrophages or type A synovial cells.

TNF-α induced expression of OX40, but not CD40L, on T cells. We recently showed that IL-1 produced by APCs induces CD40L and OX40 expression on T cells (15). It has also been reported that ligation between CD40 on APCs and CD40L on T cells leads to TNF-α production from APCs (13). Here we examined the possible involvement of TNF-α in the induction of CD40L and OX40 on T cells. When CD4$^+$ T cells from WT mice were stimulated with varying concentrations of TNF-α (1–100 ng/ml) together with plate-coated anti-CD3 mAb (0–1 μg/ml), the higher concentrations of TNF-α upregulated OX40 expression (Figure 5A), but not CD40L expression, on T cells (Figure 5B). These results suggest that TNF-α may contribute to the development of arthritis in IL-1Ra$^{-/-}$ mice through the induction of OX40 expression on T cells. However, at the highest concentration of anti-CD3 mAb (1 μg/ml), maximal expression of OX40 could occur independent of TNF-α (data not shown).

Involvement of CD40-CD40L and/or OX40-OX40L pathways in the development of arthritis. To explore the contribution of CD40-CD40L and OX40-OX40L pathways to the pathogenesis of arthritis, we injected blocking Abs for these molecules into IL-1Ra$^{-/-}$ mice. Abs for either CD40L or OX40L were injected into IL-1Ra$^{-/-}$ mice for 6 weeks, starting from before onset of the disease, and incidence of arthritis was monitored during the administration period. As shown in Figure 6, Abs for both CD40L and OX40L were able to partially suppress development of arthritis in IL-1Ra$^{-/-}$ mice. The incidence of arthritis was lower in mice treated with anti-CD40L Ab than in those treated with control Ab (hamster IgG) (Figure 6A). The induction of arthritis was delayed in mice treated with anti-OX40L Ab, and the incidence of arthritis after 6 weeks was lower than in mice treated with control Ab (rat IgG) (Figure 6C). However, once arthritis was induced, antibody treatment was ineffective. The severity score of affected mice was similar in anti-OX40L–treated mice and control Ab–treated mice, and severity was actually exacerbated in mice treated with anti-CD40L Ab (Figure 6, B and D). Thus, these results suggest that both the CD40-CD40L and OX40-OX40L pathways are involved in development of arthritis in IL-1Ra$^{-/-}$ mice.

Discussion

In this study, we have shown that the development of arthritis in IL-1Ra$^{-/-}$ mice is completely suppressed in *scid/scid* mice and that IL-1Ra$^{-/-}$ T cell transfers induce arthritis in *nu/nu* mice, suggesting a crucial role of T cells in the pathogenesis of arthritis in this model (Table 1 and Figure 1). T cells from arthritic IL-1Ra$^{-/-}$ mice induced arthritis more efficiently than those from nonarthritic mice, suggesting that arthritogenic-activated and/or memory T cells are generated in IL-1Ra$^{-/-}$ mice and involved in the development of arthritis. However, cells from both arthritic and nonarthritic IL-1Ra$^{-/-}$ mice were able to induce arthritis, supporting a T cell intrinsic defect. Interestingly, donor T cells from IL-1Ra$^{-/-}$ mice are not necessarily primed by autoantigens, because naive T cells from thymus could induce arthritis, although this took longer than with peripheral T cells that may have been preactivated. With regard to this, we have previously shown that IL-1 from APCs can activate T cells through the induction of CD40L and OX40 on T cells (15), and in the absence of IL-1Ra, even physiological levels of IL-1 activate T cells excessively, resulting in the development of autoimmunity (9). Our present data suggest that T cell–derived IL-1Ra also regulates T cell activity in an autocrine manner, although IL-1Ra is known to be produced by many other types of cells, including monocytes and macrophages in the synovial lining layer. In support of this notion, *IL-1Ra* mRNA expression was observed in unstimulated T cells at low levels but stronger expression was induced in activated T cells (Figure 3A). Thus, naive IL-1Ra$^{-/-}$ T cells transferred into *nu/nu* mice may be activated excessively by the endogenous physiological levels of IL-1 which are constitutively expressed in the joints (9), thereby becoming reactive against synovial components.

We showed that transplantation of IL-1Ra$^{-/-}$ BM cells induced arthritis in WT mice, and conversely, introduction of WT BM cells into IL-1Ra$^{-/-}$ mice completely suppressed the disease, indicating that BM cells and their derivatives are abnormal in IL-1Ra$^{-/-}$ mice (Figure 2). Since T cell progenitors are derived from BM cells, these observations are consistent with the notion that T cell dysfunction contributes to the development of autoimmunity. It should be noted, however, that WT mice that received IL-1Ra$^{-/-}$ BM cells took longer to develop arthritis than did nonarthritic IL-1Ra$^{-/-}$ mice that received the same BM cells. Thus, not only the donor BM cells, but also the recipient milieu, seems to be involved in the development of arthritis, suggesting that IL-1Ra from relatively radiation-resistant cells also plays a role. Since the time required for developing arthritis in WT mice that receive IL-1Ra$^{-/-}$ BM cells (3–4 months) is long enough to replace all the BM-derived cells in the recipient mice including the macrophages and type A synovial lining cells in the joint with donor type cells (16), this observation suggests that these late replacing components are involved in the development of arthritis. The observation that it took more than 16 weeks for arthritic IL-1Ra$^{-/-}$ mice that received normal BM cells to recover from the disease also supports this idea.

We have shown that the development of arthritis is completely suppressed in TNF-$\alpha^{-/-}$ mice, indicating a crucial role for TNF-α in the pathogenesis of RA (Figure 4). In this context, a dominant role of TNF-α in the pathogenesis of RA has been demonstrated by recent clinical trials using anti-TNF-α Ab and studies in the mouse using the CIA model (3, 18, 19). It was also reported that transgenic mice carrying the *TNF*-α gene or mice deficient for the TNF-α AU-rich element ($TNF^{\Delta ARE}$), which produce higher amounts of the TNF-α protein, develop arthritis spontaneously (7, 8). However, since $TNF^{\Delta ARE}$ mice develop arthritis even in the absence of mature lymphocytes (8), cells in the innate immune system such as neutrophils, macrophages, and mast cells, rather than the T cell–dependent immune system, have been suggested to be involved in the pathogenesis of this arthritis. Likewise, it has also been reported that inflammatory cytokines such as IL-1 and TNF-α, but not IL-6, play critical roles in the effector phase of the disease in the K/BxN model, in which arthritis can be induced by serum transfer (20). The effect of TNF-α deficiency, however, was not as strong in the CIA and K/BxN models compared to that seen in the IL-$1Ra^{-/-}$ mice. Thus, the IL-$1Ra^{-/-}$ mouse is one of the most sensitive models to the effects of TNF-α.

Cell transfers showed that TNF-$\alpha^{-/-}$ IL-$1Ra^{-/-}$ BM cells could not induce arthritis in WT recipient mice, indicating that BM-derived cells are responsible for the production of TNF-α that is crucial for the development of arthritis. Nonetheless, it is interesting that TNF-$\alpha^{-/-}$ IL-$1Ra^{-/-}$ BM cells could induce arthritis in IL-$1Ra^{-/-}$ recipient mice but not in WT recipient mice. With regard to this, TNF-α expression is augmented in IL-$1Ra^{-/-}$ mouse joints and this TNF-α may compensate for the deficiency in BM-derived cells. It is known that T cells are sensitive to irradiation and synovial lining cells are relatively resistant to irradiation, but some of the synovial lining cells such as the type A cells are of BM origin and are eventually replaced by donor cells after BM cell transplantation. Our results suggest that TNF-α is produced by these synovial lining cells in recipient IL-$1Ra^{-/-}$ mice (Figure 3E). This TNF-α may contribute to the arthritogenic milieu observed in IL-$1Ra^{-/-}$ mice in the IL-$1Ra^{-/-}$ BM cell transfer experiments. Although some $CD4^+$ T cell populations produce TNF-α, it is unlikely that TNF-α produced by these cells is the only source of TNF-α involved in the pathogenesis because, if that were true, TNF-$\alpha^{-/-}$ IL-$1Ra^{-/-}$ BM cells would not have induced arthritis even in IL-$1Ra^{-/-}$ recipient mice. However, since activated IL-$1Ra^{-/-}$ T cells produce high amounts of TNF-α (Table 2 and Figure 3E), it seems likely that T cell–derived TNF-α also contributes to the development of arthritis. Transfer of TNF-$\alpha^{-/-}$ IL-$1Ra^{-/-}$ T cells into *nu/nu* mice will help evaluate this possibility, although we were not able to address this question because of the difference in the MHC locus between the TNF-$\alpha^{-/-}$ and *nu/nu* mice.

We previously showed that IL-1 plays an important role in enhancing T cell–APC interactions by inducing CD40L and OX40 on T cells, and CD40L and OX40 expression were enhanced in T cells stimulated with antigen-bearing IL-$1Ra^{-/-}$ APCs compared to WT APCs (15). It is known that ligation of CD40 on APCs with CD40L induces OX40L expression and TNF-α production by APCs (13, 14). Here, we have shown that TNF-α induces OX40 expression on T cells (Figure 5A). Thus, the mechanism for T cell activation by IL-1 is proposed as follows. Upon interaction with antigens, APCs produce IL-1, and IL-1 activates T cells, resulting in the induction of CD40L. Then, the CD40L-CD40 interaction activates APCs to produce TNF-α. This TNF-α induces OX40 on T cells, leading to enhancement of cytokine production and activation of B cells.

IL-17 plays important roles in inflammatory diseases such as arthritis, contact hypersensitivity, asthma, and delayed-type hypersensitivity (21–23). It was recently reported that a minor subpopulation of activated $CD4^+$ T cells produces both TNF-α and IL-17 (24) and acts in synergy or additively with TNF-α and IL-1 by enhancing their production and action (25). We recently found that IL-17 production from IL-$1Ra^{-/-}$ T cells was induced by OX40 activation, and that IL-17–deficiency completely suppressed development of arthritis in IL-$1Ra^{-/-}$ mice (17). Thus, it is possible that increased OX40 expression on T cells by TNF-α may induce production of IL-17, resulting in exacerbated inflammation.

We show here that blocking CD40-CD40L and OX40-OX40L interactions inhibited the development of arthritis in IL-$1Ra^{-/-}$ mice (Figure 6). These results suggest that blocking molecules downstream of IL-1 and TNF-α in T cell activation may be effective to inhibit development of arthritis in IL-$1Ra^{-/-}$ mice. However, our results showed that once arthritis started, treatment with antibody to CD40L actually exacerbated the progression of the disease (Figure 6B). It was recently reported that activation of CD40-expressing cells has a beneficial effect on the treatment of chronic CIA (26), indicating that not only inhibition of CD40-CD40L interactions, but also CD40 ligation, can be used to reduce the autoimmune inflammatory response. Consistent with this observation, an aggressive form of polyarthritis was described in a patient with a point mutation in the *CD40L* gene (27). Thus, the CD40-CD40L system may play dual functions in the development of arthritis, and blocking the CD40-CD40L interaction by antibody treatment may also prevent beneficial effects of CD40 expression, resulting in exacerbated inflammation in IL-$1Ra^{-/-}$ mice after onset of the disease.

In summary, we have found a novel T cell regulatory mechanism in which IL-1Ra produced by T cells acts on T cells in an autocrine manner. We also showed that IL-1-induced TNF-α is crucial for the development of arthritis in IL-$1Ra^{-/-}$ mice and that this TNF-α induces OX40 on T cells. Furthermore, we showed that inhibition of either TNF-α or OX40 function is effective to suppress the development of arthritis, providing a clue for the development of new therapies for RA.

Methods

Mice. IL-$1Ra^{-/-}$ mice were produced as described (28). TNF-$\alpha^{-/-}$ mice were kindly provided from K. Sekikawa (National Institute of Agrobiological Sciences, Tsukuba, Japan). These mice were backcrossed to the BALB/c strain mice for 8 generations. BALB/c mice, BALB/c-*nu/nu* mice, and BALB/c-*scid/scid* mice were purchased from Clea. B10.D2/n (C57BL/6 congenic) mice were purchased from Japan SLC Inc. BALB.B (BALB/c congenic) mice were provided by T. Shiroishi (National Institute of Genetics, Mishima, Japan). Age- and gender-matched mice were used in each experiment. Mice were kept under specific pathogen-free conditions in an environmentally controlled clean room at the Center for Experimental Medicine, Institute of Medical Science, University of Tokyo, Japan. The animal experiments were approved by the Committee for Animal Experiments of the Institute of Medical Science, University of Tokyo. Gene manipulation experiments were carried out according to the law for such experiments.

Thymocyte, splenocyte, and T cell preparation and transfer. Donor mice for splenocyte or arthritic T cell transfer were between 8 and 12 weeks old, and those for nonarthritic T cell transfer were between 4 and 5 weeks old. Cells were prepared from spleen, thymus, and LNs (axillary, inguinal, branchial,

cervical, and popliteal) as described previously (15). For T cell purification, spleen and LN cells were washed and passed through a nylon wool column, treated with anti-mouse B220 and Mac-1 magnetic beads and passed through a MACS column (Miltenyi Biotec). Purified CD3$^+$ T cells were less than 92% CD3$^+$. Prepared cells were resuspended in 0.2 ml PBS and i.v. transferred into BALB/c-*nu/nu* mice. Numbers of transferred cells per mouse were 10^8 cells for thymocyte transfers, 4×10^7 cells for total splenocyte transfers, and 2×10^7 cells for T cell–depleted splenocyte and T cell transfers.

Incidence of arthritis and the severity score were judged macroscopically and histologically as described previously (9). Briefly, the severity score was judged by eye: grade 0 = normal, grade 1 = light swelling of the joint and/or redness of the footpad, grade 2 = obvious swelling of the joint, and grade 3 = severe swelling and fixation of the joint. The severity score was calculated for all 4 limbs, giving a maximal score of 12 points for one mouse.

BM cell preparation and transfer. Donor mice were between 4 and 8 weeks old. BM cells from femurs, tibiae, and pelves were treated with a hemolysis buffer (17 mM Tris-HCl and 140 mM NH_4Cl, pH7.2) to remove red blood cells. T cells were removed by treating with anti-mouse Thy1.2 magnetic beads and then passed through a MACS column. T cell–depleted and purified BM cells (10^7 cells) in 0.2 ml PBS were i.v. transferred into lethally irradiated (750 rad) recipient mice.

T cell activation, cytokine ELISA, and RT-PCR. CD4$^+$ T cells were purified as described (15). Purified T cells (2×10^5 cells) were plated on a 96-well plate coated with 1 or 10 μg/ml of anti-mouse CD3 mAb (145-2C11; BD Biosciences – Pharmingen) in a final volume of 200 μl RPMI1640 plus 10% FCS and cultured for 48 hours. Culture supernatant was then collected and cell proliferation was measured by incorporation of [^{3}H] thymidine (Amersham Biosciences) (15). IFN-γ, IL-4, and TNF-α levels in culture were measured by ELISA as described previously (22, 29). For the IL-1Ra ELISA, polyclonal goat anti-mouse IL-1Ra (1 μg/ml, R&D Systems Inc.) and polyclonal biotinylated goat anti-mouse IL-1Ra (2 μg/ml, R&D Systems Inc.) Abs were used as capture and detection Abs, respectively. Streptavidin-AP (SouthernBiotech) and substrate (Sigma-Aldrich) were used for detection. Recombinant mouse IL-1Ra (R&D Systems Inc.) was used as a standard. The detection limit was 3.9 pg/ml.

Total RNAs were isolated from BALB/c T cells or T cell–depleted splenocytes using Trizol reagent (Invitrogen Corp.). RNAs were denatured in the presence of oligo (dT)12-18 primer and then reverse transcribed using SuperScript (Invitrogen) at 42°C for 1 hour. PCR was performed for 30 cycles that was within log-phase amplification stages for the PCR products. The primer sequences were as follows: IL-1Ra forward primer, 5′-GACCCTGCAAGATGCAAGCC-3′; IL-1Ra reverse primer, 5′-GAGCGGATGAAGGTAAAGCG-3′; β_2m forward primer, 5′-TGACCGGCTTGTATGCTATC-3′; β_2m reverse primer, 5′-CAGTGTGAGCCAGGATATAG-3′. These IL-1Ra primers detect both secreted and intracellular forms of IL-1Ra.

Intracellular staining of cytokines. For the intracellular staining for IL-1Ra, PECs, or CD4$^+$, T cells were prepared from BALB/c or IL-1Ra$^{-/-}$ mice. PECs were stimulated with LPS (5 μg/ml) for 3 hours, followed by LPS stimulation with 2 μM monensin for 12 hours, then cells were suspended in a staining buffer (PBS containing 2% FCS and 0.01% sodium azide). After blocking with anti-FcγRII/III receptor mAb (BD Biosciences – Pharmingen), cells were treated with FITC-anti-CD11b mAb (BD Biosciences – Pharmingen). Splenocytes were stimulated with soluble anti-CD3 mAb (1 μg/ml), and purified CD4$^+$ T cells were stimulated with plate-coated anti-CD3 mAb (1 μg/ml) for 72 hours, and the GolgiPlug (BD Biosciences – Pharmingen) was added for the final 6 hours of stimulation. Cells were treated with anti-FcγRII/III receptor mAb and stained with cychrome-anti-CD4 mAb (BD Biosciences – Pharmingen). These cells were then fixed with PBS containing 4% paraformaldehyde for 20 minutes. After washing with a permeabilization buffer (PBS containing 10 mM HEPES, 0.1% BSA, and 0.5% Triton X-100), cells were incubated with goat anti-mouse IL-1Ra Ab (R&D Systems Inc.) or isotype-matched control Ab (goat IgG; R&D Systems Inc.) in the permeabilization buffer for 30 minutes at 4°C. Cells were then washed with the permeabilization buffer and stained with Cy5-donkey-anti-goat IgG (Jackson ImmunoResearch Laboratories).

For intracellular cytokine staining for IFN-γ, IL-4, and TNF-α, synovial tissues were dissected from the ankle joints of IL-1Ra$^{-/-}$ mice who had already developed arthritis and normal ankle joints of WT mice. These joints were digested in a cocktail of 2.4 mg/ml hyaluronidase (Sigma-Aldrich), 1 mg/ml collagenase (Wako Pure Chemical Industries) and 100 μg/ml DNase I (Sigma-Aldrich) in RPMI plus 10% FBS for 1.5 hours at 37°C. The cells were filtered through a nylon mesh, washed with RPMI plus 10% FBS, then stimulated with PMA (10 ng/ml) and Ionomycin (400 ng/ml; Sigma-Aldrich) for 6 hours at 37°C with 2 μM monensin. These cells were blocked with anti-FcγRII/III receptor mAb and stained with cell lineage–specific Abs against cell surface molecules, then fixed in 4% paraformaldehyde for 20 minutes, resuspended in the permeabilization buffer, and stained with anti-cytokine Abs for 45 minutes at 4°C. Abs used for the cell lineage-specific staining were as follows: FITC-anti-CD11b, allophycocyanin-anti-TCR-β, CyChrome-anti-CD4, and allophycocyanin-anti-CD8 (BD Biosciences – Pharmingen). Those used for intracellular staining were as follows: PE-anti-IFN-γ, PE-anti-IL-4 (BD Biosciences – Pharmingen), and PE-anti-TNF-α (eBioscience). Cells were washed with the permeabilization buffer and analyzed using FACSCalibur by CellQuest software (BD).

Flow cytometric analysis of costimulatory molecules. CD40L and OX40 expression on CD4$^+$ T cells was analyzed as described previously (15). Briefly, for CD40L expression, purified CD4$^+$ T cells on 12-well plates (1×10^6 cells/well) were stimulated with plate-coated anti-CD3 mAb with or without mouse recombinant TNF-α (Peprotech) in the presence of 1 μg of biotinylated anti-mouse CD40L mAb (MR-1; BD Biosciences – Pharmingen) or biotinylated hamster IgG (eBioscience) as an isotype-matched control Ab for 24 hours. For OX40 expression, CD4$^+$ T cells were stimulated with plate-coated anti-CD3 mAb with or without TNF-α for 72 hours. Cells were stained with allophycocyanin-anti-mouse-CD4 mAb (PharMingen) and either biotinylated anti-mouse OX40 mAb (OX86, eBioscience) or biotinylated rat IgG (eBioscience), followed by staining with PE-streptavidin (BD Biosciences – Pharmingen).

Antibody preparation and treatment. Anti-OX40L Ab and anti-CD40L Ab were produced in hybridoma cell lines, MGP34 and MR-1, respectively. For OX40L Ab preparation, hybridoma cells were allowed to proliferate in ascites of *nu/nu* mice for 7–10 days or cultured in serum-free medium with the iMAb Monoclonal Antibody Production Kit (Diagnostic Chemicals Ltd.) for 4 weeks. Ascites and culture supernatant was collected and Abs were purified using Protein A column (Amersham Biosciences). For CD40L Ab preparation, hybridoma cells were cultured in serum-free medium for 4 weeks. Supernatant was collected and Abs were purified using Protein G column (Amersham Biosciences). Anti-OX40L Ab (500 μg) or anti-CD40L Ab (250 μg) was intraperitoneally injected into nonarthritic IL-1Ra$^{-/-}$ mice twice a week for 6 weeks. Rat IgG or hamster IgG (Cappel, ICN Pharmaceuticals) was injected as the isotype control for anti-OX40L or anti-CD40L Ab, respectively. Mice treated with Abs were between 4 and 6 weeks old. Arthritic score was inspected at the time of Ab injection.

Statistics. The repeated-measures ANOVA–Fisher's protected least significant different test (post hoc test) or the chi-square test for independence was used for statistical evaluation of incidence. The 2-way ANOVA was used for statistical evaluation of the arthritic score. The statistical significance of affected mice scores was calculated from the point at which 2 or more mice of each genotype became arthritic. The Student's *t* test was used for statistical evaluation of the results except for incidence and score.

Acknowledgments

We thank K. Sekikawa for TNF-$\alpha^{-/-}$ mice, T. Shiroishi for BALB.B mice, S. Mori and T. Nakajima (University of Tokyo, Tokyo, Japan) for histological sections, and S.J. Galli (Stanford University School of Medicine, Stanford, California, USA) for support in the experiments. We also thank all the members of the lab for their discussion and help in animal care. This work was supported by grants from the Ministry of Education, Culture, Sport, and Science of Japan; the Ministry of Health and Welfare of Japan; CREST; the Japan Society for the Promotion of Science; and the Japan Rheumatism Foundation.

Received for publication December 5, 2003, and accepted in revised form October 5, 2004.

Address correspondence to: Yoichiro Iwakura, Center for Experimental Medicine, Institute of Medical Science, University of Tokyo, Shirokanedai, Minato-ku, Tokyo 108-8639, Japan. Phone: 81-3-5449-5536, Fax: 81-3-5449-5430; E-mail: iwakura@ims.u-tokyo.ac.jp.

Susumu Nakae's present address is: Department of Pathology, Stanford University School of Medicine, Stanford, California, USA.

Taizo Matsuki's present address is: Japan Science and Technology Agency, Tokyo, Japan.

Katsuko Sudo's present address is: Animal Research Center, Tokyo Medical University, Tokyo, Japan.

1. Feldmann, M., Brennan, F.M., and Maini, R.N. 1996. Role of cytokines in rheumatoid arthritis. *Annu. Rev. Immunol.* **14**:397–440.
2. Firestein, G.S., and Zvaifler, N.J. 1992. Rheumatoid arthritis: a disease of disordered immunity. In *Inflammation: basic principles and clinical correlates.* 2nd edition. J.I. Gallin, I.M. Goldstein, and R. Snyderman, editors. Raven Press, Ltd. New York, New York, USA. 959–975.
3. Feldmann, M., and Maini, R.N. 2001. Anti-TNF-α therapy of rheumatoid arthritis: what have we learned? *Annu. Rev. Immunol.* **19**:163–196.
4. Tocci, M.J., and Schmidt, J.A. 1997. Interleukin-1: Structure and function. In *Cytokines in health and disease.* 2nd edition. D.G. Remick and J.S. Friedland, editors. Marcel Dekker, Inc. New York, New York, USA. 1–27.
5. Iwakura, Y. 2002. Roles of IL-1 in the development of rheumatoid arthritis: consideration from mouse models. *Cytokine Growth Factor Rev.* **13**:341–355.
6. Arend, W.P., Malyak, M., Guthridge, C.J., and Gabay, C. 1998. Interleukin-1 receptor antagonist: role in biology. *Annu. Rev. Immunol.* **16**:27–55.
7. Kollias, G., Douni, E., Kassiotis, G., and Kontoyiannis, D. 1999. On the role of tumor necrosis factor and receptors in models of multiorgan failure, rheumatoid arthritis, multiple sclerosis and inflammatory bowel disease. *Immunol. Rev.* **169**:175–194.
8. Kontoyiannis, D., Pasparakis, M., Pizarro, T.T., Cominelli, F., and Kollias, G. 1999. Impaired on/off regulation of TNF biosynthesis in mice lacking TNF AU-rich elements: implications for joint and gut-associated immunopathologies. *Immunity.* **10**:387–398.
9. Horai, R., et al. 2000. Development of chronic inflammatory arthropathy resembling rheumatoid arthritis in interleukin 1 receptor antagonist-deficient mice. *J. Exp. Med.* **191**:313–320.
10. Niki, Y., et al. 2001. Macrophage- and neutrophil-dominant arthritis in human IL-1α transgenic mice. *J. Clin. Invest.* **107**:1127–1135.
11. Mima, T., et al. 1995. Transfer of rheumatoid arthritis into severe combined immunodeficient mice. The pathogenetic implications of T cell populations oligoclonally expanding in the rheumatoid joints. *J. Clin. Invest.* **96**:1746–1758.
12. Weinberg, A.D. 1998. Antibodies to OX-40 (CD134) can identify and eliminate autoreactive T cells: implications for human autoimmune disease. *Mol. Med. Today.* **4**:76–83.
13. van Kooten, C., and Banchereau, J. 2000. CD40-CD40 ligand. *J. Leukoc. Biol.* **67**:2–17.
14. Weinberg, A.D. 2002. OX40: targeted immunotherapy – implications for tempering autoimmunity and enhancing vaccines. *Trends Immunol.* **23**:102–109.
15. Nakae, S., Asano, M., Horai, R., Sakaguchi, N., and Iwakura, Y. 2001. IL-1 enhances T cell-dependent antibody production through induction of CD40 ligand and OX40 on T cells. *J. Immunol.* **167**:90–97.
16. Kitagawa, H., et al. 1993. Analyses of origin of synovial cells and repairing mechanisms of arthritis by allogeneic bone marrow transplantation. *Immunobiology.* **188**:99–112.
17. Nakae, S., et al. 2003. IL-17 production from activated T cells is required for the spontaneous development of destructive arthritis in mice deficient in IL-1 receptor antagonist. *Proc. Natl. Acad. Sci. U. S. A.* **100**:5986–5990.
18. Thorbecke, G.J., et al. 1992. Involvement of endogenous tumor necrosis factor α and transforming growth factor β during induction of collagen type II arthritis in mice. *Proc. Natl. Acad. Sci. U. S. A.* **89**:7375–7379.
19. Joosten, L.A., et al. 1999. IL-1αβ blockade prevents cartilage and bone destruction in murine type II collagen-induced arthritis, whereas TNF-α blockade only ameliorates joint inflammation. *J. Immunol.* **163**:5049–5055.
20. Ji, H., et al. 2002. Critical roles for interleukin 1 and tumor necrosis factor α in antibody-induced arthritis. *J. Exp. Med.* **196**:77–85.
21. Lubberts, E., et al. 2001. IL-1-independent role of IL-17 in synovial inflammation and joint destruction during collagen-induced arthritis. *J. Immunol.* **167**:1004–1013.
22. Nakae, S., et al. 2002. Antigen-specific T cell sensitization is impaired in IL-17-deficient mice, causing suppression of allergic cellular and humoral responses. *Immunity.* **17**:375–387.
23. Nakae, S., Nambu, A., Sudo, K., and Iwakura, Y. 2003. Suppression of immune induction of collagen-induced arthritis in IL-17-deficient mice. *J. Immunol.* **171**:6173–6177.
24. Infante-Duarte, C., Horton, H.F., Byrne, M.C., and Kamradt, T. 2000. Microbial lipopeptides induce the production of IL-17 in Th cells. *J. Immunol.* **165**:6107–6115.
25. Chabaud, M., and Miossec, P. 2001. The combination of tumor necrosis factor alpha blockade with interleukin-1 and interleukin-17 blockade is more effective for controlling synovial inflammation and bone resorption in an ex vivo model. *Arthritis Rheum.* **44**:1293–1303.
26. Mauri, C., Mars, L.T., and Londei, M. 2000. Therapeutic activity of agonistic monoclonal antibodies against CD40 in a chronic autoimmune inflammatory process. *Nat. Med.* **6**:673–679.
27. Webster, E.A., et al. 1999. An aggressive form of polyarticular arthritis in a man with CD154 mutation (X-linked hyper-IgM syndrome). *Arthritis Rheum.* **42**:1291–1296.
28. Horai, R., et al. 1998. Production of mice deficient in genes for interleukin (IL)-1α, IL-1β, IL-1α/β, and IL-1 receptor antagonist shows that IL-1β is crucial in turpentine-induced fever development and glucocorticoid secretion. *J. Exp. Med.* **187**:1463–1475.
29. Nakae, S., Asano, M., Horai, R., and Iwakura, Y. 2001. Interleukin-1β, but not interleukin-1α, is required for T-cell-dependent antibody production. *Immunology.* **104**:402–409.

Available online at www.sciencedirect.com
ScienceDirect
Vaccine 25 (2007) 630–637
Vaccine
www.elsevier.com/locate/vaccine

SARS-CoV spike protein-expressing recombinant vaccinia virus efficiently induces neutralizing antibodies in rabbits pre-immunized with vaccinia virus

Masahiro Kitabatake[a,b], Shingo Inoue[c], Fumihiko Yasui[a], Shoji Yokochi[a,d], Masaaki Arai[a,e], Kouichi Morita[c], Hisatoshi Shida[f], Minoru Kidokoro[g], Fukashi Murai[d], Mai Quynh Le[h], Kyosuke Mizuno[i], Kouji Matsushima[b], Michinori Kohara[a,*]

[a] *Department of Microbiology and Cell Biology, The Tokyo Metropolitan Institute of Medical Science, 3-18-22, Honkomagome, Bunkyo-ku, Tokyo 113-8613, Japan*
[b] *Department of Molecular Preventive Medicine, School of Medicine, The University of Tokyo, 7-3-1, Hongo, Bunkyo-ku, Tokyo 113-0033, Japan*
[c] *Department of Virology, Institute of Tropical Medicine, Nagasaki University, 1-12-4, Sakamoto, Nagasaki 852-8523, Japan*
[d] *Post Genome Institute Co., Ltd., 3-38-1, Hongo, Bunkyo-ku, Tokyo 113-0033, Japan*
[e] *Pharmaceuticals Research Unit, Research & Development Division, Mitsubishi Pharma Corporation, 1000, Kamoshida-cho, Aoba-ku, Yokohama 227-0033, Japan*
[f] *Division of Molecular Virology, Institute for Genetic Medicine, Hokkaido University, N15 W7, Kita-ku, Sapporo 060-0815, Japan*
[g] *Third Department of Virology, National Institute of Infectious Diseases, 4-7-1, Gakuen, Musashimurayama 208-0011, Japan*
[h] *Department of Virology, National Institute of Hygiene and Epidemiology, Hanoi, Vietnam*
[i] *The Chemo-Sero-Therapeutic Research Institute, 1-6-1, Okubo, Kumamoto 860-8568, Japan*

Received 15 May 2006; received in revised form 20 July 2006; accepted 19 August 2006
Available online 11 September 2006

Abstract

A vaccine for severe acute respiratory syndrome (SARS) is being intensively pursued against its re-emergence. We generated a SARS coronavirus (SARS-CoV) spike protein-expressing recombinant vaccinia virus (RVV-S) using highly attenuated strain LC16m8. Intradermal administration of RVV-S into rabbits induced neutralizing (NT) antibodies against SARS-CoV 1 week after administration and the NT titer reached 1:1000 after boost immunization with RVV-S. Significantly, NT antibodies against SARS-CoV were induced by administration of RVV-S to rabbits that had been pre-immunized with LC16m8. RVV-S can induce NT antibodies against SARS-CoV despite the presence of NT antibodies against VV. These results suggest that RVV-S may be a powerful SARS vaccine, including in patients previously immunized with the smallpox vaccine.

Keywords: SARS coronavirus; Recombinant vaccinia virus; LC16m8

1. Introduction

In November 2002, an influenza-like acute pneumonia designated as severe acute respiratory syndrome (SARS) by the World Health Organization, first emerged in China and spread to 29 countries within a few months. By July 2003, 8098 probable cases with 774 deaths were reported (www.cdc.gov/mmwr/mguide_sars.html). The etiologic agent of SARS was identified as a novel type of coronavirus (CoV) that was genetically distinct from previously characterized members of the Coronaviridae family [1–3]. Like other coronaviruses, SARS-CoV is a positive stranded RNA virus with an approximately 30 kb genome encoding non-structural proteins as well as structural proteins, including spike, envelope, membrane and nucleocapsid. Spike protein is a type I transmembrane glycoprotein that mediates binding to the host cell receptor using an amino-terminal S1

* Corresponding author. Tel.: +81 3 4463 7589; fax: +81 3 3828 8945.
E-mail address: mkohara@rinshoken.or.jp (M. Kohara).

0264-410X/$ – see front matter © 2006 Elsevier Ltd. All rights reserved.
doi:10.1016/j.vaccine.2006.08.039

domain and membrane fusion using a carboxyl-terminal S2 domain [4]. Angiotensin-converting enzyme 2 (ACE2) binds to the S1 domain of SARS-CoV spike protein and functions as a receptor for SARS-CoV [5]. CoV spike protein is a major target of protective immunity [6], and neutralizing (NT) antibodies and cytotoxic T lymphocytes against SARS-CoV spike protein have been detected in SARS patients [7,8]. These findings indicate that SARS-CoV spike protein is an appropriate target for vaccines and therapy.

The SARS epidemic broke in May 2003. However, several cases of SARS were reported in China in 2004. Although the civet cat and bats are suspected to be the natural hosts of SARS-CoV, the reservoir of SARS-CoV has yet to be identified [9–11]. In addition, the precise mechanism underlying the development of SARS is not clear and the therapeutic guidelines for SARS have not been established. It has been reported that prophylactic and therapeutic treatment with pegylated IFN-α reduces viral replication and excretion in SARS-CoV infected macaques [12]. Although pegylated IFN-α may eventually become a good therapeutic agent for SARS after infection, it cannot provide long-term protection when used as a prophylactic agent. Therefore, the development of a SARS vaccine is imperative. Several groups have reported a number of SARS vaccine candidates, including inactivated SARS-CoV vaccines [13,14], DNA vaccines [15,16] and recombinant viral vaccines [17–19] expressing one or more SARS-CoV structural proteins. Recombinant live viral vaccines can generally induce strong and long-term immunity, similar to an attenuated live vaccine, and can be abundantly manufactured in a short period of time. More importantly, a safe vaccine can be developed using an attenuated strain that has already been proven safe.

Vaccinia virus (VV) is a double stranded DNA virus with an approximately 180 kb genome, and attenuated strains have been used as the smallpox vaccine. A long DNA fragment is able to be inserted into the VV genome by homologous recombination without damaging viral integrity, as the VV genome is large and contains genes non-essential for viral replication. In fact, recombinant VV can express various proteins encoded by the transduced gene, including the glycosylated proteins of pathogens, some of which have been evaluated as candidates for prophylactic and therapeutic vaccines [20]. Lister is the attenuated VV strain that was used in the worldwide smallpox eradication program. However, additional attenuated strains were generated from Lister due to its side effects, which included erythema, fever and encephalitis. LC16m8 was isolated from Lister via the intermediate strains, LC16 and LC16mO, by multiple plaque purification in primary rabbit kidney cells. LC16m8 is characterized by temperature sensitivity and the formation of small pocks [21]. No serious side effects were observed among the over 100,000 people who were immunized with LC16m8, while the immunogenicity of LC16m8 is similar to that of Lister [22]. Therefore, LC16m8 was authorized as the vaccine against smallpox by the Japanese Ministry of Health and Welfare in 1975.

Recombinant VV expresses proteins encoded by transduced genes under the control of its own promoters. Highly efficient hybrid promoters have been developed and are composed of poxvirus A-type inclusion body (ATI) late promoter and tandem repeats of mutated 7.5 kDa protein (p7.5) early promoter [23]. The protein expressed under the control of the ATI/p7.5 hybrid promoter strongly induces both humoral and cellular immunity [24]. In the present study, we generated a recombinant VV expressing SARS-CoV spike protein (RVV-S) under the control of the ATI/p7.5 hybrid promoter, using LC16m8, and examined whether RVV-S could be used as a SARS vaccine.

2. Materials and methods

2.1. Viruses and cells

SARS-CoV (Vietnam/NB-04/2003 strain), which was isolated from nasal and throat swabs from 1 patient in Hanoi, has been previously described [25]. LC16m8 and LC16mO were kindly provided by the Chemo-Sero-Therapeutic Research Institute (Kumamoto, Japan). The RK13 cell line (ATCC: CCL-37) and VERO E6 cell line (ATCC: CRL-1586) were cultured in MEM (Nissui Pharmaceutical Co. Ltd., Tokyo, Japan) containing 5% fetal bovine serum.

2.2. Generation of recombinant vaccinia virus

The pSFJ1-10 vector contains the ATI/p7.5 hybrid promoter within the hemagglutinin (HA) gene region of VV [23]. Full length cDNA encoding the SARS-CoV spike protein gene was cloned from SARS-CoV viral RNA by RT-PCR, and then inserted downstream of the ATI/p7.5 hybrid promoter of pSFJ1-10; final designation: pSFJ1-10-SARS-S. pSFJ1-10-SARS-S was then transfected into RK13 cells that had been infected with LC16m8 at a multiplicity of infection (moi) of 10 plaque forming units (PFU)/cell. At 24 h after transfection, the virus was harvested. HA negative plaques were cloned as described previously [26]. Briefly, the harvested virus was re-infected into RK13 cells. At 96 h after infection, cells were washed with PBS (+) twice, and then incubated with chicken erythrocytes for 30 min at 30 °C. Following washing again with PBS (+), white plaques were isolated. Isolated viruses were cloned by three serial rounds of plaque purification using erythrocyte agglutination and then propagated in RK13 cells. Insertion of the SARS-CoV spike protein gene into LC16m8 genome was confirmed by direct PCR and expression was detected by Western blotting. The viral titer of RVV-S was determined using the standard plaque assay.

2.3. Western blotting

RK13 cells were infected with RVV-S or LC16m8 at moi 10. After 24 h infection, cells were lysed with RIPA

Table 1
Immunization schedule of RVV-S and LC16m8

Rabbit #	0 week		6 weeks		12 weeks		18 weeks	
	Virus	Dose (PFU)	Virus	Dose (PFU)	Virus	Dose (PFU)	Virus	Dose (PFU)
R1–R3	RVV-S	10^8	RVV-S	10^8				
R4–R6	LC16m8	10^8	LC16m8	10^8	RVV-S	10^8	RVV-S	10^8
R7–R9	RVV-S	10^6	RVV-S	10^6				
R10–R12	RVV-S	10^7	RVV-S	10^7				
R13–R15	LC16m8	10^7	RVV-S	10^7	RVV-S	10^7		

buffer (10 mM Tris, pH 7.4, 150 mM NaCl, 1% SDS and 0.5% Nonidet-P40), and 30 μg of total protein was subjected to 7.5% SDS-PAGE and was transferred to a polyvinylidene difluoride membrane (Immobilon-P, Millipore, Bedford, MA). The membrane was blocked in 5% skim milk in TBS containing 0.1% Tween-20 (TBS-T) and then washed with TBS-T. Polyclonal antibodies against spike protein were used as the primary antibody. These were prepared from rabbit sera immunized with a KLH-conjugated spike protein peptide (amino acid residues 559–570 or 1236–1248) and the IgG fraction purified using the Ampure PA kit (Amersham Bioscience, Piscataway, NJ). Antigen-antibody interaction was detected by horseradish peroxidase (HRP)-conjugated donkey anti-rabbit polyclonal antibodies (Amersham Bioscience) and visualized using the ECL system (Amersham Bioscience).

2.4. Immunofluorescence analysis

RK13 cells seeded on slide-glass were infected with RVV-S or LC16m8 at moi 5. At 12 h after incubation at 30 °C, cells were fixed in cold acetone/methanol and then blocked in 1% BSA in PBS (−) for 1 h at room temperature. Following removal of the blocking buffer, cells were incubated with polyclonal antibodies against spike protein, which recognize the C-terminal peptide of spike protein (amino acid residues 1236–1248), for 1 h at room temperature. Following three washes with PBS containing 0.05% Tween-20 (PBS-T), cells were incubated with Alexa 488-conjugated anti-rabbit IgG (Invitrogen, Carlsbad, CA) for 1 h at room temperature. After washing again with PBS-T, the slide-glasses were mounted in Permafluor (Beckman Coulter, Fullerton, CA) containing 1 μg/ml 6-diamidino-2-phenylindole (DAPI) and analyzed using a confocal microscope (LSM510, Carl Zeiss, Oberkochen, Germany).

2.5. Immunization of rabbits

Groups of three New Zealand White rabbits, which were purchased from SLC (Hamamatsu, Japan), were intradermally immunized with one of several doses (10^6, 10^7 or 10^8 PFU) of RVV-S, or with 10^8 PFU of LC16m8, at 0 and 6 weeks. The LC16m8 immunized group was further immunized with 10^8 PFU of RVV-S at 12 and 18 weeks. Another group of three rabbits was immunized with 10^7 PFU of LC16m8 at 0 week, and then immunized with 10^7 PFU of RVV-S at 6 and 12 weeks. A summary of the immunization schedule is shown in Table 1. Sera were collected every week, and used for enzyme linked immunosorbent assay (ELISA) and the *in vitro* neutralization (NT) assay below. All animal experiments were approved by The Tokyo Metropolitan Institute of Medical Science Animal Experiment Committee and were performed in accordance with the animal experimentation guidelines of The Tokyo Metropolitan Institute of Medical Science.

2.6. ELISA

Full length recombinant SARS-CoV spike protein containing a six-histidine tag (His) was expressed in RK13 cells by RVV-S-His, which was generated from LC16mO, and purified using Nickel sepharose (Amersham Bioscience). Peptides from the N-terminal (mixture of three peptides, amino acid residues 12–53, 90–115 and 171–203), middle position (mixture of two peptides, amino acid residues 408–470 and 540–573) and C-terminal (mixture of three peptides, amino acid residues 1051–1076, 1121–1154 and 1162–1190) of the spike protein, which respond to sera from SARS-infected individuals, were purchased from ProSpec-Tany TechnoGene Ltd. (Rehovot, Israel). These three peptide mixtures or full length spike protein were coated onto the 96 well plates at 4 °C. The plates were blocked with 1% BSA in PBS (−) containing 0.5% Tween-20 and 2.5 mM EDTA, and then incubated with serial dilutions of sera from the rabbits immunized with RVV-S or LC16m8. After extensive washing, the plates were incubated with HRP-conjugated donkey anti-rabbit polyclonal antibodies (Amersham Bioscience). Antigen–antibody interactions were detected using 3,3′,5,5′-tetramethylbenzidine solution as the substrate (Becton Dickinson, San Jose, CA), and the binding activity was measured by the absorbance at 450 nm.

2.7. In vitro NT assay for SARS-CoV

Serial dilutions of heat-inactivated sera were mixed with equal volumes of 100 $TCID_{50}$ of SARS-CoV and incubated at 37 °C for 1 h. VERO E6 cells were then infected with the virus/sera mixtures in 96 well plates. At 120 h after infection, the NT titer was determined as the maximum dilution of sera that inhibited the SARS-CoV induced cytopathic effect by more than 50%. All experiments with SARS-CoV were performed in a biosafety containment level III facility.

2.8. In vitro NT assay for VV

Serial dilutions of heat-inactivated sera were mixed with equal volumes of 100 PFU of LC16mO, and incubated at 37 °C for 1 h, followed by incubation at 4 °C for 16 h. RK13 cells were then infected with the virus/sera mixtures in 6 well plates. At 48 h after infection, the NT titer was determined as the maximum dilution of sera that inhibited plaque formation by more than 50%.

2.9. Statistical analysis

All data were expressed as mean ± S.E.M. Data for RVV-S dose dependent effect were statistically analyzed by one-way ANOVA followed by Turkey test. Data for LC16m8 pre-immunization effect were statistically analyzed by Student's or by Welch's t-test. $p < 0.05$ was considered to be statistically significant.

3. Results

3.1. Generation and characterization of RVV-S

The full length SARS-CoV spike protein gene was inserted by homologous recombination into the HA gene region of LC16m8, which was located downstream of the powerful ATI/p7.5 hybrid promoter (Fig. 1A). Recombination between pSFJ1-10-SARS-S and LC16m8 results in inactivation of the HA gene. We screened for RVV-S using the erythrocyte agglutination assay, and insertion of the transduced gene was then confirmed by PCR. To confirm the expression of SARS-CoV spike protein, Western blotting was performed. Two kinds of rabbit polyclonal antibodies that recognized different epitopes, amino acid residues 559–570 and 1236–1248 of SARS-CoV spike protein, were used as the primary antibody. In RVV-S but not LC16m8 infected cells, both antibodies detected an approximately 180 kDa protein (Fig. 1B and C), which is consistent with the molecular mass of spike protein [18]. SARS-CoV spike protein is reported to be highly glycosylated, and thus the molecular mass on SDS-PAGE is larger than that predicted from the gene sequence [18]. Expression of spike protein following infection with RVV-S was also confirmed by immunofluorescence analysis. RVV-S infected VERO E6 cells were stained with antibody against spike protein, whereas no staining was observed in the cells infected with LC16m8 or the uninfected control cells (Fig. 1D).

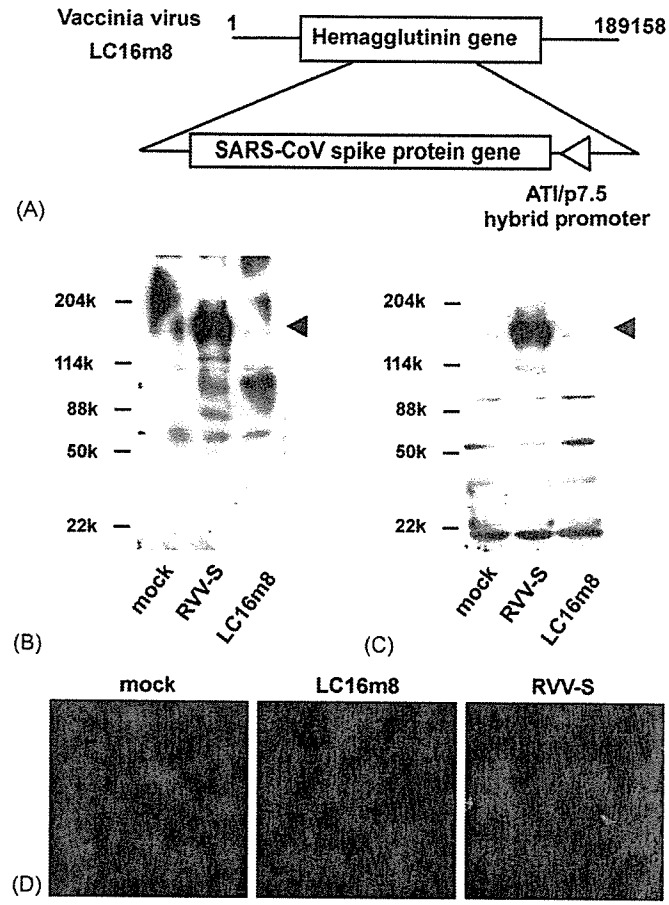

Fig. 1. Characteristics of SARS-CoV spike protein-expressing recombinant vaccinia virus (RVV-S) derived from LC16m8. (A) The full length SARS-CoV spike protein gene was inserted into the HA gene region of the LC16m8 genome. The ATI/p7.5 hybrid promoter regulates expression of spike protein. (B and C) RK13 cells were infected with RVV-S or LC16m8 at moi 10. At 24 h after infection, cells were harvested and analyzed. Two kinds of anti-SARS-CoV spike protein polyclonal antibodies, which recognize different epitopes, namely amino acid residues 559–570 (B) and 1236–1248 (C) of spike protein, were used as the primary antibodies. The molecular masses of marker proteins in kDa are shown on the left and the position of the spike protein is indicated by an arrowhead on the right. (D) Indirect immunofluorescence staining of spike protein. Expression of spike protein was visualized by staining with anti-SARS-CoV spike polyclonal antibodies, followed by Alexa 488-conjugated anti-rabbit IgG (green). Nuclei were stained with DAPI (red).

3.2. Induction of binding antibodies against spike protein in RVV-S-immunized rabbits

To investigate whether RVV-S induces binding antibodies against spike protein, 10^8 PFU of RVV-S or LC16m8 (as the control) was intradermally injected into rabbits at 0 and 6 weeks. Rabbits immunized with either RVV-S or LC16m8 did not exhibit weight loss or any clinical signs except for regional skin reactions, such as erythema and induration. The skin reaction induced by RVV-S was comparable to that induced by LC16m8 (data not shown). Binding antibodies against full length spike protein were detected by ELISA in the sera from rabbits immunized with RVV-S (Fig. 2A). Next, we investigated the binding activities of immunized sera against different epitopes of the spike protein. RVV-S-immunized sera reacted with all three regions of spike protein. The sera bound to the C-terminal peptides, which contained the heptad repeat 2 (HR2) region, reported to be the NT epitope of SARS-CoV (Fig. 2B) [27] and to the middle peptides,

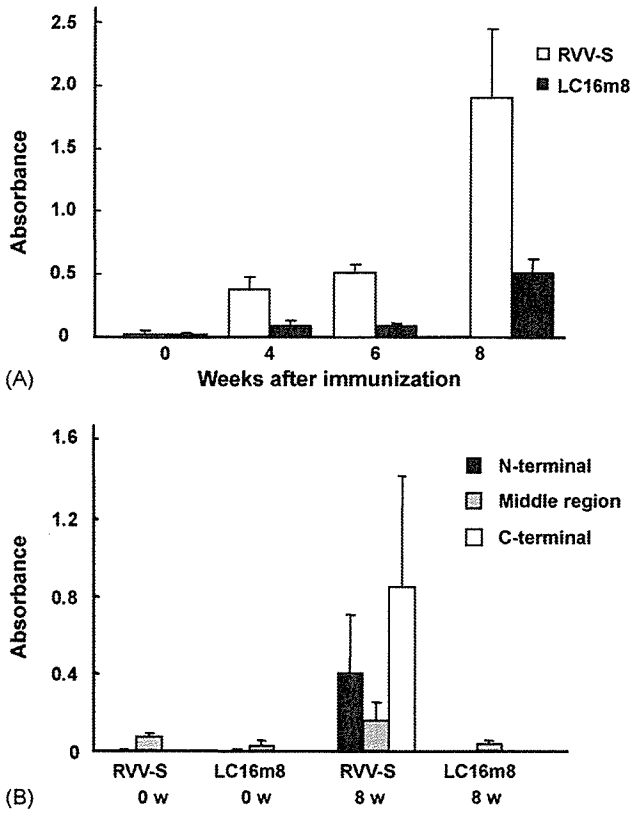

Fig. 2. Induction of binding antibodies against SASR-CoV spike protein. New Zealand White rabbits ($n = 3$) were immunized with 10^8 PFU of RVV-S (R1-3; open symbols) or LC16m8 (R4–6; closed symbols) at 0 and 6 weeks. The binding activity of 10^3- or 10^4-fold dilutions of immunized sera was assessed using His-tagged full length spike protein (A), or one of three kinds of spike protein partial peptides (B), as the capture antigen.

in which a receptor binding domain, another NT epitope of SARS-CoV, was included [28].

3.3. Induction of NT antibodies against SARS-CoV in RVV-S-immunized rabbits

Next, to determine whether the antibodies induced by immunization with RVV-S have NT activity against SARS-CoV, we performed an *in vitro* NT assay against SARS-CoV using immunized sera. Interestingly, the sera obtained from all three rabbits in this group showed NT activity against SARS-CoV, even at 1 week after immunization with 10^8 PFU of RVV-S (Fig. 3A). The NT titer reached 1:100 at 3 weeks, and increased 10-fold further by boost immunization. In contrast, sera obtained from rabbits immunized with LC16m8 did not show any NT activity against SARS-CoV (Fig. 3A). Next, to determine the minimum dose that can induce NT antibodies against SARS-CoV by single immunization, rabbits were immunized with lower doses of RVV-S. All three rabbits that underwent single immunization with 10^7 PFU of RVV-S generated NT antibodies against SARS-CoV (Fig. 3A). The NT titer further increased by boost immunization with 10^7 PFU of RVV-S and reached a comparable level to that induced by 10^8 PFU of RVV-S (Fig. 3B). On the other hand, NT activity was induced by single immunization with 10^6 PFU of RVV-S at 2 and 4 weeks after immunization in all three rabbits, but then decreased below the detection limit in one rabbit at 6 weeks (Fig. 3A). However, the NT titer increased to approximately 1:300 in the group immunized with 10^6 PFU of RVV-S by boost immunization with the same dose of RVV-S (Fig. 3B).

3.4. RVV-S induces NT antibodies against SARS-CoV in the presence of NT antibodies against VV

Induction of NT antibodies against VV by RVV-S was next examined. The *in vitro* NT assay against VV revealed that LC16m8 and RVV-S equally induced NT antibodies against VV in the rabbits (Fig. 3C). NT activity against VV was induced by 10^8 PFU of RVV-S at 1 week after immunization, similar to SARS-CoV. The NT titer against VV, which reached 1:10,000 at 2 weeks after boost immunization with 10^8 PFU of RVV-S, was similar to that induced by 10^8 PFU of LC16m8. These results suggest that the epitopes of the NT antibodies against VV were preserved in RVV-S. Since VV has been used as a smallpox vaccine in humans, we were concerned that RVV-S might be eliminated by the host's immune response before inducing effective immunity against a protein encoded by the transduced gene. Therefore, to assess whether RVV-S can induce NT antibodies against SARS-CoV in rabbits that had NT antibodies against VV, RVV-S was injected into rabbits which had been pre-immunized with LC16m8. NT antibodies against VV were induced in the rabbits by single immunization with 10^7 PFU of LC16m8 and the NT titer reached 1:64–256 (Fig. 4A). By following immunization with an equal dose of RVV-S (10^7 PFU), NT antibodies against SARS-CoV were induced in all three rabbits, although induction of NT antibodies was delayed in one rabbit (R14). Although the induction of NT antibodies against SARS-CoV was partially suppressed in the LC16m8 pre-immunized rabbits, the NT titer further increased in all three rabbits by boost immunization with RVV-S (Fig. 4C). These results suggest that RVV-S can induce NT antibodies in individuals who have been previously immunized with a smallpox vaccine. Next, we examined whether RVV-S induced NT antibodies against SARS-CoV in rabbits with a high titer of NT antibodies against VV. The NT titer against VV in rabbits that had been immunized twice with 10^8 PFU of LC16m8 was sustained at approximately 1:4000 (Fig. 4B). Although these rabbits had an extremely high titer of NT antibodies against VV, NT antibodies against SARS-CoV were induced in all three rabbits upon a booster injection with 10^8 PFU of RVV-S (Fig. 4B). Surprisingly, the NT titer of these rabbits increased to levels comparable to those of the non-pre-immunized rabbits (Fig. 4C). These results indicate that an immune response against a protein encoded by a transduced gene can be induced by immunization with 10^8 PFU of RVV in spite of the pre-existence of NT antibodies against VV.

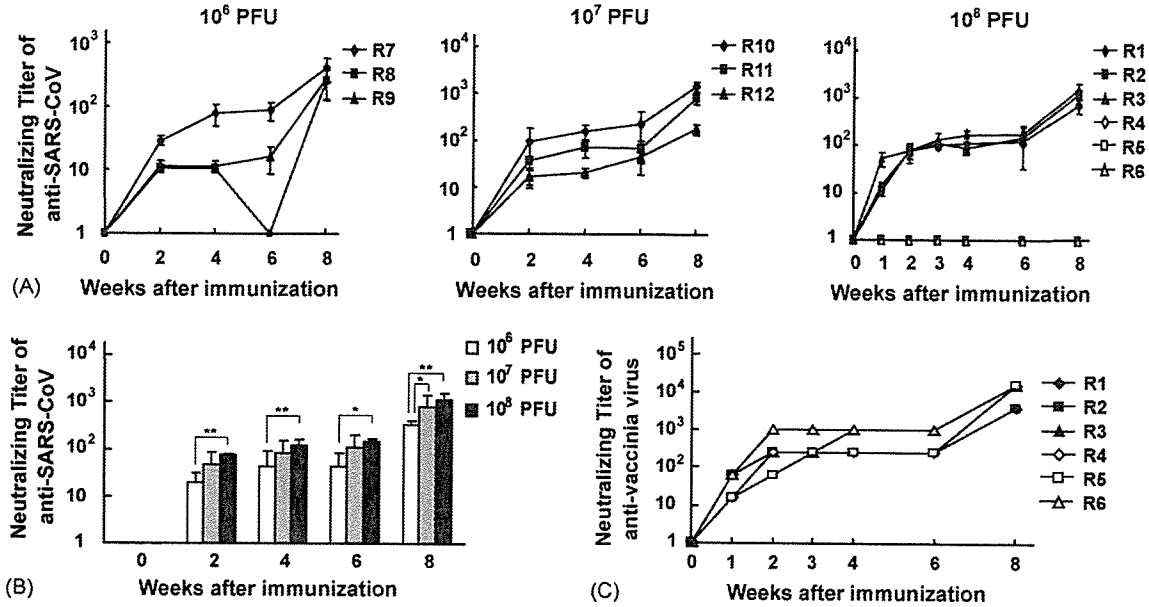

Fig. 3. Induction of NT antibodies against SARS-CoV and vaccinia virus. (A) The NT activity against SARS-CoV of RVV-S- (10^6 PFU, R7–9; 10^7 PFU, R10–12; 10^8 PFU, R1–3; closed symbols) or 10^8 PFU of LC16m8- (R4–6; open symbols) immunized rabbit sera was defined as the maximum dilution of sera that inhibited the cytopathic effect of SARS-CoV by more than 50%. (B) The dose dependency of immunization with RVV-S shown in (A). $^*p<0.05$, $^{**}p<0.01$. (C) The NT activity against vaccinia virus of RVV-S- (R1–3, closed symbols) or LC16m8- (R4–6, open symbols) immunized sera was defined as the maximum dilution of sera that inhibited plaque formation by LC16mO by more than 50%.

4. Discussion

In the present study, we generated a SARS-CoV spike protein-expressing recombinant vaccinia virus using a highly attenuated strain, LC16m8, and demonstrated that NT antibodies against SARS-CoV can be strongly induced by immunization with RVV-S, not only in naïve rabbits but also in LC16m8 pre-immunized rabbits.

In a previous study, passive transfer of sera obtained from mice inoculated with SARS-CoV prevented the replication of SARS-CoV in the upper and lower respiratory tract [29]. In addition, intraperitoneal injection of sera from mice immunized with MVA expressing spike protein (MVA/S) reduced the viral titers in lung and nasal turbinate in a dose-dependent manner [18]. These finding indicate that NT antibodies against spike protein are sufficient to protect against SARS-CoV infection. Single immunization with 10^7 or 10^8 PFU of RVV-S and two immunizations with 10^6 PFU of RVV-S were able to induce a high level of NT antibodies against SARS-CoV at 2 weeks after immunization. Therefore, RVV-S also may protect against SARS-CoV *in vivo* and would be a highly effective vaccine against SARS in naïve individuals.

Contrary to the above studies [18,29], Czub et al. [30] reported that immunization with MVA/S did not prevent SARS-CoV infection in ferrets but rather produced inflammatory responses and focal necrosis in the liver after SARS-CoV challenge. This may have been due to only low NT activity against SARS-CoV being induced by the MVA/S immunization. Moreover, the precise mechanism of this liver inflammation has not been clarified. Feline infectious peritonitis virus (FIPV), another member of the coronaviruses, exhibited enhanced FIPV infection into monocytes/macrophages through viral-specific antibody binding to the Fc receptors of these cells, and caused enhanced inflammation [31]. However, there is no evidence that NT antibodies against SARS-CoV cause antibody-dependent enhancement, and correlation between inflammation and antibody-dependent enhancement by MVA/S vaccination has not yet been established. The side effects of vaccines are also influenced by the dosage and route of immunization. In Czub's report, MVA/S was intraperitoneally injected into the ferrets, although most vaccinations with RVV are conducted through other routes, such as intradermal, intramuscular or subcutaneous injection. Therefore, selection of a different immunization route may prevent such side effects. Nonetheless, further analysis of the side effects of various SARS vaccines, including RVV-S, is required in *in vivo* SARS-CoV challenge models in a variety of animals.

Using RVV-S as a candidate SARS vaccine means that possible complications due to previous vaccination with the VV for smallpox may be avoided. Hammarlund et al. [32] reported that a particular antiviral antibody against poxvirus is maintained for a very long time (possibly for life) by immunization with the smallpox vaccine. Therefore, there was concern that a RVV vaccine would be eliminated by the host antiviral immune response before induction of effective humoral and/or cellular immunity against the protein encoded by the transduced gene. However, immunization with 10^7 PFU of RVV-S induced NT antibodies against SARS-CoV in rabbits that had been immunized with 10^7 PFU